


Provided for non-commercial research and education use.
Not for reproduction, distribution or commercial use.

Volume 55 Number 11 November 2008 ISSN 0967-0637	
	DEEP-SEA RESEARCH
Editor: Michael P. Bacon Woods Hole, MA, USA	PART I
Oceanographic Research Papers	
A. MANTZIAFOU and A. LASCARATOS	1403 Deep-water formation in the Adriatic Sea: Interannual simulations for the years 1979–1999
D.A. LEONOV and W.K. DEWAR	1428 On nonlinear baroclinic trapped waves over abrupt topography
M.E. BAIRD, P.G. TIMKO, J.H. MIDDLETON, T.J. MULLANEY, D.R. COX and I.M. SUTHERS	1438 Biological properties across the Tasman Front off southeast Australia
F. NOT, M. LATASA, R. SCHAREK, M. VIPREY, P. KARLESKIND, V. BALAGUÉ, I. ONTORIA-OVIEDO, A. CUMINO, E. GOETZE, D. VAULOT and R. MASSANA	1456 Protistan assemblages across the Indian Ocean, with a specific emphasis on the picoeukaryotes
I.G. PRIEDE, A. JAMIESON, A. HEGER, J. CRAIG and A.F. ZUUR	1474 The potential influence of bioluminescence from marine animals on a deep-sea underwater neutrino telescope array in the Mediterranean Sea
R.S. LAMPITT, B. BOORMAN, L. BROWN, M. LUCAS, I. SALTER, R. SANDERS, K. SAW, S. SEEVAVE, S.J. THOMALLA and K. TURNEWITSCH	1484 Particle export from the euphotic zone: Estimates using a novel drifting sediment trap, ²²² Rn and new production
A.K. SWEETMAN and U. WITTE	1503 Macrofaunal response to phytodetritus in a bathyal Norwegian fjord
V. SURUGIU, J.-C. DAUVIN, P. GILLET and T. RUELLET	1515 Can seamounts provide a good habitat for polychaete annelids? Example of the northeastern Atlantic seamounts
C. FONTANIER, E.J. JORISSEN, B. LANSARD, A. MOURET, R. BUSCAIL, S. SCHIMDT, P. KERHERVÉ, F. BURON, S. ZARAGOSI, G. HUNAULT, E. ERNOULT, C. ARTERO, P. ANSCHUTZ and C. RABOUILLE	1532 Live foraminifera from the open slope between Grand Rhône and Petit Rhône Canyons (Gulf of Lions, NW Mediterranean)
S. JENSEN, J.D. NEUFELD, N.-K. BIRKELAND, M. HOVLAND and J.C. MURRELL	1554 Insight into the microbial community structure of a Norwegian deep-water coral reef environment
<i>(Contents continued on outside back cover)</i>	
www.elsevier.com/locate/dsri	

This article appeared in a journal published by Elsevier. The attached copy is furnished to the author for internal non-commercial research and education use, including for instruction at the authors institution and sharing with colleagues.

Other uses, including reproduction and distribution, or selling or licensing copies, or posting to personal, institutional or third party websites are prohibited.

In most cases authors are permitted to post their version of the article (e.g. in Word or Tex form) to their personal website or institutional repository. Authors requiring further information regarding Elsevier's archiving and manuscript policies are encouraged to visit:

<http://www.elsevier.com/copyright>



Contents lists available at ScienceDirect

Deep-Sea Research I

journal homepage: www.elsevier.com/locate/dsri

Protistan assemblages across the Indian Ocean, with a specific emphasis on the picoeukaryotes

Fabrice Not^{a,*}, Mikel Latasa^{b,c}, Renate Scharek^c, Manon Viprey^a, Pierre Karleskind^{a,1},
Vanessa Balagué^b, Imelda Ontoria-Oviedo^b, Andrea Cumino^b, Erica Goetze^d,
Daniel Vaultot^a, Ramon Massana^b

^a Station Biologique de Roscoff, UMR7144 Centre National de la Recherche Scientifique (CNRS), Institut National des Sciences de l'Univers (INSU) et Université Pierre et Marie Curie, Place George Teissier, 29680 Roscoff, France

^b Institut de Ciències del Mar (CMIMA-CSIC), Passeig Marítim de la Barceloneta 37–49, E-08003 Barcelona, Spain

^c Centro Oceanográfico de Gijón (IEO), Avenida Príncipe de Asturias 70bis, E-33212 Gijón-Xixón, Spain

^d Department of Marine Ecology and Aquaculture, Danish Institute for Fisheries Research, Kavalergården 6, DK-2920 Charlottenlund, Denmark

ARTICLE INFO

Article history:

Received 4 October 2007

Received in revised form

20 June 2008

Accepted 25 June 2008

Available online 28 June 2008

Keywords:

Protist

Phytoplankton

Picoplankton

Diversity

Indian Ocean

ABSTRACT

Protists, and among them the picoeukaryotes (cells < 3 μm), have been described as significant contributors to both carbon biomass and production in oligotrophic regions of the oceans. However, protist assemblages remain largely undescribed in pelagic ecosystems and in particular in the Indian Ocean. In the present work, we investigated protists along an eastward transect across the sub-tropical gyre of the Indian Ocean (from South Africa to Australia), with a particular focus on picoeukaryotes. We combined inverted and epifluorescence microscopy, flow cytometry, pigment analysis, denaturing gel gradient electrophoresis (DGGE), 18S rDNA clone libraries, and fluorescent *in situ* hybridization (FISH). Overall the picophytoplankton fraction contributed 88% and 90% of total Chl *a* at the surface and DCM, respectively, with picoeukaryotes accounting for 38% and 50% of total Chl *a* at the surface and DCM. Considering only the Indian South Subtropical Gyre (ISSG) province, we observed greater shifts in the picoeukaryotic assemblage throughout the upper 200 m of the water column than along the ca. 10,000 km cruise track. In terms of taxonomic diversity and contribution of each taxon to the picoeukaryotic community, prasinophytes were well represented at more coastal stations with the genus *Micromonas* reaching densities up to 750 cell mL⁻¹ in coastal waters and less than 100 cell mL⁻¹ at open ocean stations. Haptophytes (56% and 45% of picoeukaryotic pigments at surface and DCM, respectively) and possibly pelagophytes (28% and 40% of picoeukaryotic pigments at surface and DCM, respectively) appeared to be dominant at open ocean stations. Other groups and in particular organisms affiliated to chrysophytes, and to a lesser extent to cryptophytes, appear as clear targets for future qualitative and quantitative studies. Moreover, the occurrence of many sequences related to radiolarians (5% and 27% at surface and DCM, respectively) will require further investigation.

© 2008 Elsevier Ltd. All rights reserved.

* Corresponding author. Tel.: +33 932 309 500.

E-mail address: not@sb-roscoff.fr (F. Not).

¹ Present address: Laboratoire des Sciences de l'Environnement Marin (LEMAR), Institut Universitaire Européen de la Mer, UMR 6539 CNRS/Université de Bretagne Occidentale, Place Nicolas Copernic 29280 Plouzané, France.

1. Introduction

Protistan assemblages can be categorized according to conventional taxonomic classification or to size fractions (Sieburth et al., 1978). The importance of picoplankton

(defined here as cells $<3\mu\text{m}$) has been primarily emphasized in oligotrophic areas of the oceans, where they participate in nutrient remineralization (Azam et al., 1983) and may contribute up to 95% of the primary production (Raven, 1998). Among the three classically recognized groups of picophytoplankton, *Prochlorococcus*, *Synechococcus*, and picoeukaryotes, the latter usually have the lowest numerical abundance. Nevertheless, the importance of picoeukaryotes in terms of biomass and primary productivity has been demonstrated for various marine pelagic ecosystems (Li, 1994; Marañón et al., 2001; Worden et al., 2004). Early studies of photosynthetic picoeukaryotic diversity in the open ocean were based mostly on pigment analysis. These investigations suggested haptophytes and pelagophytes as significant components of the community, while green algae and other groups were less frequently observed (Ondrusek et al., 1991; Letelier et al., 1993; Andersen et al., 1996). Nevertheless, green algae and more specifically prasinophytes can be significant in particular locations or under certain conditions (Suzuki et al., 2002). Since 2001, molecular techniques have been applied to qualitatively describe the diversity of picoeukaryotes in the open ocean (Díez et al., 2001b; López García et al., 2001; Moon-van der Staay et al., 2001). Our first insights into the abundance and distribution of particular taxa (i.e. *Micromonas pusilla*, Prasinophytes) were obtained in coastal environments (Biéga et al., 2003; Not et al., 2004; Countway and Caron, 2006), and few data (qualitative or quantitative) are currently available from oligotrophic regions of the open ocean.

Although the Indian Ocean gyre is one of the largest oligotrophic areas of the world ocean, it has received far less attention than gyres of the northern Atlantic and Pacific Oceans. Only the Arabian Sea in the north-western Indian Ocean (north of 10°S latitude), which is strongly influenced by monsoonal winds, has been subjected to several international interdisciplinary programs (e.g. the 1994–1996 Arabian Sea Expedition: Oceanic Response to Monsoonal Forcing; Smith et al., 1998). In those studies, picoplankton was shown to contribute 35–92% of phytoplanktonic chlorophyll *a* (Chl *a*) in transects from the coast towards the oligotrophic open ocean (Latasa and Bidigare, 1998; Brown et al., 1999). The abundance and contribution of picoeukaryotes to biomass was more important at coastal nutrient-rich stations than in oligotrophic areas, where *Prochlorococcus* dominated (Campbell et al., 1998; Latasa and Bidigare, 1998; Brown et al., 1999). Molecular approaches investigating the diversity of photosynthetic picoeukaryotes in the Arabian Sea demonstrated the prominent contribution of chrysophyte and prymnesiophyte algae (Fuller et al., 2006a,b). Extensive regions south of the Arabian Sea, including the oceanic gyre in the Southern hemisphere, remain poorly known.

In the present study we characterized the diversity of microbial eukaryotic assemblages along an eastward transect across the subtropical Indian Ocean gyre from South Africa to Australia. Because of the expected dominance of picoplankton in the planktonic community of oligotrophic areas, we focused our investiga-

tions on this size fraction and, more specifically, on the picoeukaryotes (both heterotrophs and phototrophs), for which assemblages in the open ocean remain poorly described. In order to achieve a comprehensive view of the system, we used a multi-technique approach, combining tools routinely used to assess eukaryotic microbial diversity: inverted and epifluorescence microscopy, flow cytometry, molecular fingerprinting (DGGE: denaturing gel gradient electrophoresis), 18S rDNA clone libraries, pigment analysis, and fluorescent *in situ* hybridization with taxon specific probes. Comparisons across techniques allowed us to observe both general patterns and the fine scale structure of assemblages.

2. Materials and methods

2.1. Sampling

The oceanographic cruise VANC10MV took place during late austral fall (15 May–13 June 2003) on board the oceanographic vessel R/V *Melville* (Scripps Institution of Oceanography, UCSD). Fourteen stations were sampled to assess the diversity of phytoplankton along an eastward transect from Cape Town (South Africa), through the subtropical Indian Ocean, to Port Hedland (Australia) (Fig. 1 and Table 1). Temperature, salinity, and *in situ* fluorescence profiles were obtained by CTD casts at each station (Sea-Bird Electronics 911 Plus, Bellevue, WA). CTD sensor data were processed according to standard Sea-Bird recommendations for each instrument, and subsequently included in a 10-m-depth binned final data file. Vertical profiles of *in vivo* fluorescence were corrected for background offset and converted to Chl *a* concentration using a regression of extracted Chl *a* concentrations as measured by fluorometry against *in vivo* fluorescence at all depths and stations sampled ($n = 83$, slope = 0.66, $R^2 = 0.77$). Seawater samples were collected using 15 L Niskin bottles mounted on a rosette. At each station, five to seven depths were selected for sampling based on real-time hydrological and fluorescence profiles obtained from the CTD sensors. Three levels were consistently sampled: surface (5 m), the deep chlorophyll maximum (DCM), and the layer below the DCM (200 m). One or two additional samples were collected between the surface and DCM, one between the DCM and 200 m and one mesopelagic sample (650–1000 m depth). Seawater was pre-filtered through a $200\mu\text{m}$ mesh prior to further analyses.

2.2. Flow cytometry (FCM)

Seawater samples (1.5 mL, total and $<3\mu\text{m}$ size fraction) were fixed with a mix of glutaraldehyde and paraformaldehyde (0.1% and 1% final concentration, respectively). Triplicate samples for each size fraction were subsequently deep frozen in liquid nitrogen and stored at -80°C for long-term storage. Samples were processed using a FACSort flow cytometer (Becton Dickinson, San José, CA), and cells enumerated following the protocol described by Marie et al. (1999).

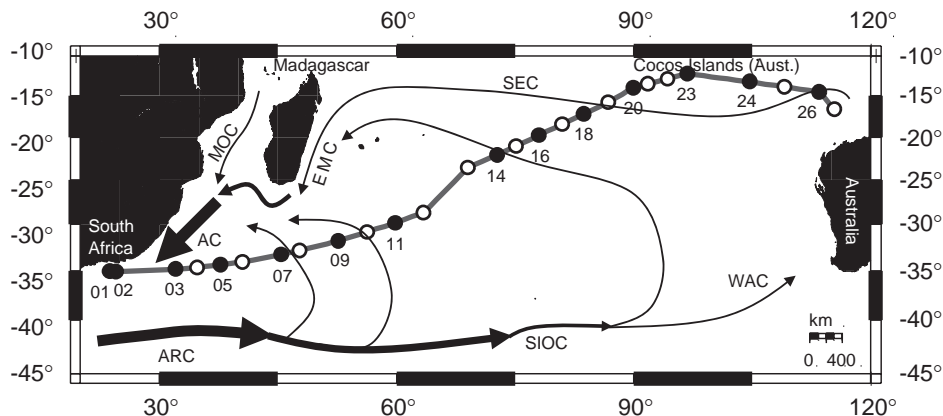


Fig. 1. Cruise track and station locations during the eastward transect from South Africa (Cape Town) to Australia (Port Hedland), across the subtropical gyre of the Indian Ocean. Black dots and associated numbers indicate the stations sampled for the present study. Surface circulation is adapted from (Stramma and Lutjeharms, 1997): Agulhas Return Current (ARC), South Indian Ocean Current (SIOC), West Australia Current (WAC), South Equatorial Current (SEC), East Madagascar Current (EMC), Mozambique Current (MOC), and Agulhas Current (AC). Surface chlorophyll data for the sampled period can be retrieved at <http://oceancolor.gsfc.nasa.gov/cgi/level3.pl>.

2.3. Epifluorescence microscopy

Samples for epifluorescence microscopy were fixed with ice-cold glutaraldehyde (1% final concentration), stained with 4,6-diamidino-2-phenylindole (DAPI; $5 \mu\text{g mL}^{-1}$ final concentration) and filtered on $0.6 \mu\text{m}$ pore-size black polycarbonate filters. Filters were mounted on a slide with low fluorescence oil and kept frozen until laboratory enumeration of microorganisms, within one month after the cruise, using an Olympus BX61 microscope. Protists (unicellular eukaryotes) were discriminated from prokaryotes and counted by standard epifluorescence microscopy based on their blue fluorescence under UV excitation (Caron, 1983). Total protist counts were separated into two categories, heterotrophic and phototrophic cells, based on the absence or presence of red fluorescence from chlorophyll under blue light excitation. Moreover, organisms were classified into three size classes (<3 , $3\text{--}5$, $>5 \mu\text{m}$) by visual measurements using an ocular micrometer.

2.4. Inverted microscopy

Samples were fixed with hexamine-buffered formaldehyde (0.6% final concentration). Diversity and abundance of nano- and microplankton were determined using the Utermöhl technique (Utermöhl, 1958). Analysis was performed with an inverted microscope (Zeiss Axiovert). In order to classify phytoplankton into ecological categories, diatoms were divided into $<20 \mu\text{m}$ (nanoplanktonic) and $>20 \mu\text{m}$ (microplanktonic) size groups. The latter group contained all chain-forming species. Coccolithophorids were divided into <10 and $>10 \mu\text{m}$ cell size groups. Because of the size spectrum of coccolithophorids, a separation at $10 \mu\text{m}$ appeared more adequate. Autotrophic and heterotrophic species of dinoflagellates were divided into size classes of <20 , $20\text{--}30$, $30\text{--}50$, and $>50 \mu\text{m}$, and ciliates were divided into size classes of <30 , $30\text{--}50$, and $>50 \mu\text{m}$.

2.5. Fluorescent *in situ* hybridization

Sample preparation (i.e. fixation and filtration) was performed on $<3 \mu\text{m}$ pre-filtered sea water. Fluorescent *in situ* hybridization was performed either directly on board or in the laboratory, according to the procedure described in Not et al. (2002). The group-specific oligonucleotide probes used in this study were (1) a mix of EUK1209R, CHLO01, and NCHLO01 probes in order to target all eukaryotes; (2) probe CHLO02, specific for chlorophytes; (3) probe PRYM02, specific for haptophytes; and (4) probes MICRO01, BATHY01, and OSTREO01, which are specific for the genera *Micromonas*, *Bathycoccus*, and *Ostreococcus* (Mamiellales, Prasinophytae), respectively. Hybridized samples were observed under epifluorescence microscopy (Olympus BX51). Counts of hybridized cells were performed either from 15 randomly chosen ocular grids (when more than ca. 10 cells per $100 \times 100 \mu\text{m}$ grid were observed) or from two transects across the section of filter observed (when cell densities were lower). Based on hybridization replicates, we estimated an error of 27% ($n = 24$) for samples where more than $100 \text{ cells mL}^{-1}$ were detected and of 65% ($n = 15$) for samples where less than $100 \text{ cells mL}^{-1}$ were detected. High-quality FISH hybridizations were prevented by a white precipitate (probably from the fixative) on the filters from stations 20 to 26 and, therefore, only results for stations 01–18 are presented.

2.6. Sampling for DNA and denaturing gradient gel electrophoresis (DGGE)

Microbial organisms were collected on $0.2 \mu\text{m}$ Sterivex units (Millipore, Durapore) by filtering approximately 15 L of seawater through both a $3 \mu\text{m}$ pore-size polycarbonate pre-filter and the Sterivex unit in succession with a peristaltic pump, at filtration rates of $50\text{--}100 \text{ mL min}^{-1}$. The Sterivex units were filled with lysis buffer (40 mM EDTA, 50 mM Tris-HCl and 0.75 M sucrose) and frozen

Table 1

Location, characteristics, and techniques applied at each sampling station (FCM = flow cytometry; HPLC = high performance liquid chromatography; DGGE = denaturing gel gradient electrophoresis; FISH = fluorescent *in situ* hybridization; DAPI, 4'6-diamidino-2-phenylindole staining, epifluorescence counts)

Stations	Coordinates south-east	Bottom depth (m)	Surface salinity (psu)	Surface temperature (°C)	Inverted microscopy ^a	FCM ^a	HPLC ^a	DGGE ^a transect	DGGE ^a depth profile	Clone libraries ^a	FISH ^a	DAPI ^a
01	35°03'–23°44'	711	35.37	20.89	5, 25	5, 25, 35 100, 200	5, 25	5, 25	5, 25, 35 100, 200, 650	5, 25	5, 25, 35 100, 200	5, 25, 35 100, 200
02	35°03'–24°34'	1472	35.36	24.04		5, 35, 50 100, 200	5, 35	5, 35			5, 35, 50 100, 200	
03	35°49'–32°02'	3010	35.68	21.23		5, 35, 75 100, 200	5, 35	5, 35			5, 35, 75 100, 200	
05	34°21'–37°41'	5139	35.75	20.80		5, 50, 85 110, 200	5, 85	5, 85			5, 50, 85 110, 200	
07	33°17'–45°21'	1244	35.73	20.91		5, 50, 85 120, 200	5, 85	5, 85			5, 50, 85 120, 200	5, 50, 85 120, 200
09	31°49'–52°36'	4762	35.62	21.57	5, 75	5, 45, 75 120, 200	5, 75	5, 75	5, 45, 74 120, 200, 800	5, 75	5, 45, 75 120, 200	5, 45, 75 120, 150, 200
11	29°51'–59°50'	3482	35.68	21.76		5, 50, 100 130, 200	5, 100	5, 100			5, 50, 100 130, 200	
14	22°05'–72°44'	3806	35.27	24.12	1, 120	45, 90, 120 150, 200	1, 120	1, 120			45, 90, 120 150, 200	1, 45, 90, 120 150, 200
16	19°44'–78°00'	5230	34.67	25.84		50, 80, 100 120, 200	50, 100	50, 100			50, 80, 100 120, 200	
18	17°10'–83°40'	5646	34.94	25.24	5, 85	5, 50, 85 110, 200	5, 85	5, 85	5, 50, 85 110, 200, 1000	5, 85	5, 50, 85 110, 200	5, 50, 85 110, 200
20	13°57'–89°55'	5035	34.23	27.43		5, 50, 100 120, 200	5, 100	5, 100				
23	12°13'–96°47'	1440	34.03	28.48	5, 75	5, 50, 75 110, 200	5, 75	5, 75	5, 50, 75, 110, 200, 1000	5, 75		5, 50, 75 110, 200
24	13°11'–104°41'	5792	33.87	27.96		5, 50, 85 120, 200	5, 85	5, 85				
26	14°29'–113°27'	2804	34.27	27.66	5, 70	5, 50, 70 85, 100	5, 70	5, 70				5, 50, 70 100, 200

^a Numbers given correspond to sampling depth (m).

at -70°C . Cell lysis was performed by digestion with lysozyme followed by proteinase K and SDS treatments. DNA was purified by phenol/chloroform extraction and concentrated with a Centricon-100 (Millipore) as previously described (Díez et al., 2001a). DNA integrity was checked by agarose gel electrophoresis, and nucleic acid extracts were stored at -70°C until analysis.

One microliter of DNA extract was used as template for PCR (polymerase chain reaction) amplification of a 560 bp (base pair) fragment of the 18S rRNA gene using primers Euk1A and Euk516r-GC (Díez, et al., 2001a). Denaturing gradient gel electrophoresis was carried out with a DGGE-2000 system (CBS Scientific Company) as previously described (Díez et al., 2001a). Gels of 6% polyacrylamide were prepared with a gradient of denaturant agent from 40% to 65% (100% denaturant agent being 7 M urea and 40% deionized formamide). Eight hundred nanograms of PCR product were loaded for each sample and the gel was run at 100 V for 16 h at 60°C in $1 \times$ TAE buffer (40 mM Tris (pH 7.4), 20 mM sodium acetate, 1 mM EDTA). The gel was stained with SybrGold (Molecular Probes) and DNA fragments were visualized with a Fluor-S Multimaginer (Bio-Rad). High-resolution images were analyzed with the software Quantity One (Bio-Rad) to detect DGGE bands, quantify their intensity, and identify the same band position across the lanes of the gel. A matrix was constructed with the presence and relative intensity of individual bands (logarithmically normalized) in each lane. This matrix was used to calculate a distance matrix (City-block distance method) and a dendrogram using Ward's method in Statistica 6.0 (StatSoft, Inc.).

2.7. Gene clone libraries

The 18S rRNA genes were PCR amplified using the eukaryotic primer set EukA and EukB, which amplify the complete gene (ca. 1780 bp; Díez et al., 2001b). Polymerase chain reaction products from several reactions were pooled and cleaned with the QIAGEN PCR purification kit and cloned using the TOPO-TA cloning kit (Invitrogen). Presence of the 18S rRNA gene insert in positive colonies was checked by PCR amplification with the same primers. Clones with the correct insert size were sequenced directly using the BigDye Terminator Cycle Sequencing kit v.3.0 (PE Biosystems) and an ABI PRISM model 377 (v. 3.3) automated sequencer using the internal primer Euk528f (Elwood et al., 1985). The basic phylogenetic affiliation of clones was obtained by BLAST search (Altschul et al., 1997). The comparison of BLAST search results carried out using distinct portions of each individual clone led to the identification of 31 chimeras out of 572 sequences. Sequences have been deposited in GenBank under accession numbers EU561664–EU562177.

2.8. HPLC pigment analysis

Phytoplankton composition was studied using pigment markers as indicators. Chl *a*, an indicator for total phytoplankton biomass, refers to the sum of monovinyl (MVChl *a*) and divinyl (DVChl *a*) Chl *a* throughout the

paper. The *Prochlorococcus* contribution to Chl *a* was estimated directly as DVChl *a*, its pigment signature. The contribution of major groups to bulk MVChl *a* was quantified using Chemtax (Mackey et al., 1996). To obtain reliable results, Chemtax must be applied only to data in which pigment ratios within the different groups are invariant. In order to identify groups of samples with similar pigment ratios, we proceeded in the following way: (i) Pigment/Chl *a* ratios were calculated. (ii) The data were log transformed using the natural logarithm (ratios with a value equal to zero because pigment concentration was below the detection limit, were replaced by 1/3 of the minimum value for the whole data set prior to log transformation, in order to avoid undefined values). (iii) Cluster analyses were performed with the Statistica software package using the modified pigment/Chl *a* ratios of the following pigments: DVChl *c*₃, Chl *c*₂, peridinin, 19'-butanoyloxyfucoxanthin, fucoxanthin, prasinocanthin, violaxanthin, 19'-hexanoyloxyfucoxanthin, diadinoxanthin, alloxanthin, zeaxanthin and DVChl *a* (Ward's method and City-block distances). Chemtax was applied to each of the three subsets of samples with linkage distances larger than 1000 as shown in Fig. 8 (St01 surface was added to the closest set) to obtain the contribution of seven phytoplankton groups to the bulk MVChl *a*: haptophytes, pelagophytes, prasinophytes, *Synechococcus*, cryptophytes, dinoflagellates, and diatoms.

Because zeaxanthin occurs in both *Synechococcus* and *Prochlorococcus* and only the former contribute to MVChl *a*, it is necessary to distinguish between ZeaxSyn and ZeaxPro. We partitioned Zeax as $\text{ZeaxFCM} = \text{Zeax/Syn} \times [\text{Syn}]_{\text{FCM}} + \text{Zeax/Pro} \times [\text{Pro}]_{\text{FCM}}$, where Zeax/Syn and Zeax/Pro are the Zeax content cell⁻¹ of *Synechococcus* and *Prochlorococcus*, respectively, and [Syn]FCM and [Pro]FCM were the *Synechococcus* and *Prochlorococcus* cell concentrations obtained from FCM for the same sample. Initial values for Zeax/Syn and Zeax/Pro were estimated by minimizing $\sum (\text{Zeax}_{\text{HPLC}} - \text{Zeax}_{\text{FCM}})^2$ using the function Solver of Microsoft Excel in default mode (time = 100 s, iterations = 100, precision = 0.000001, tolerance = 5, convergence = 0.0001, linear estimation, progressive derivative, Newton's method). We used 0.5 fg Zeax/Pro and 1.0 Zeax/Syn as seed values.

Chemtax was applied following the procedures described in Latasa (2007) using version 1.95 of Chemtax (S. Wright, personal communication). Random pigment to Chl *a* ratios between 0.1 and 1 were used as seed values of 16 input matrices. Chemtax was run using the following parameters: ratio limits = 500, initial step size = 10, step ratio = 1.03, epsilon limit = 0.000001, cutoff step = 3,000,000, iteration limit = 250 (only the first run, 120 for all others), elements varied = 12 (no. of pigments), sub-iterations = 1, weighting = bound relative (10, as defined in the program). The output of each run was used as input for the following run and this procedure was repeated three to four times. Another set of 16 random matrices was generated and run as the first set of matrices. This procedure was repeated twice more for a final result of 64 matrices. The median of each pigment ratio was incorporated to the final pigment ratio matrix. This matrix was then used to

estimate the contribution of the different groups to MVChl *a* stock.

2.9. Taxonomic considerations

In order to avoid confusion and be consistent throughout the paper, we have chosen to use common adjectives to refer to the taxonomic groups investigated. However, those adjectives do not refer to a precise taxonomic classification. The correspondence between the terms used and the taxonomic groups defined recently by Adl et al. (2005) is presented in Supplementary Table 1.

3. Results

3.1. Hydrology, physical environment

The mean circulation of the Southern Indian Ocean is peculiar because of the geography of this basin. Unlike the Atlantic and Pacific Oceans, the Indian Ocean is completely closed on its north side and open on its east side, permitting water inflow from the equatorial Pacific, which significantly influences the hydrology of its southern sections (Reason et al., 1996). Important re-circulations from the Agulhas Return (ARC) and the South Indian Ocean (SIOC) currents are observed (Fig. 1). Based on temperature and salinity data (Fig. 2), two major

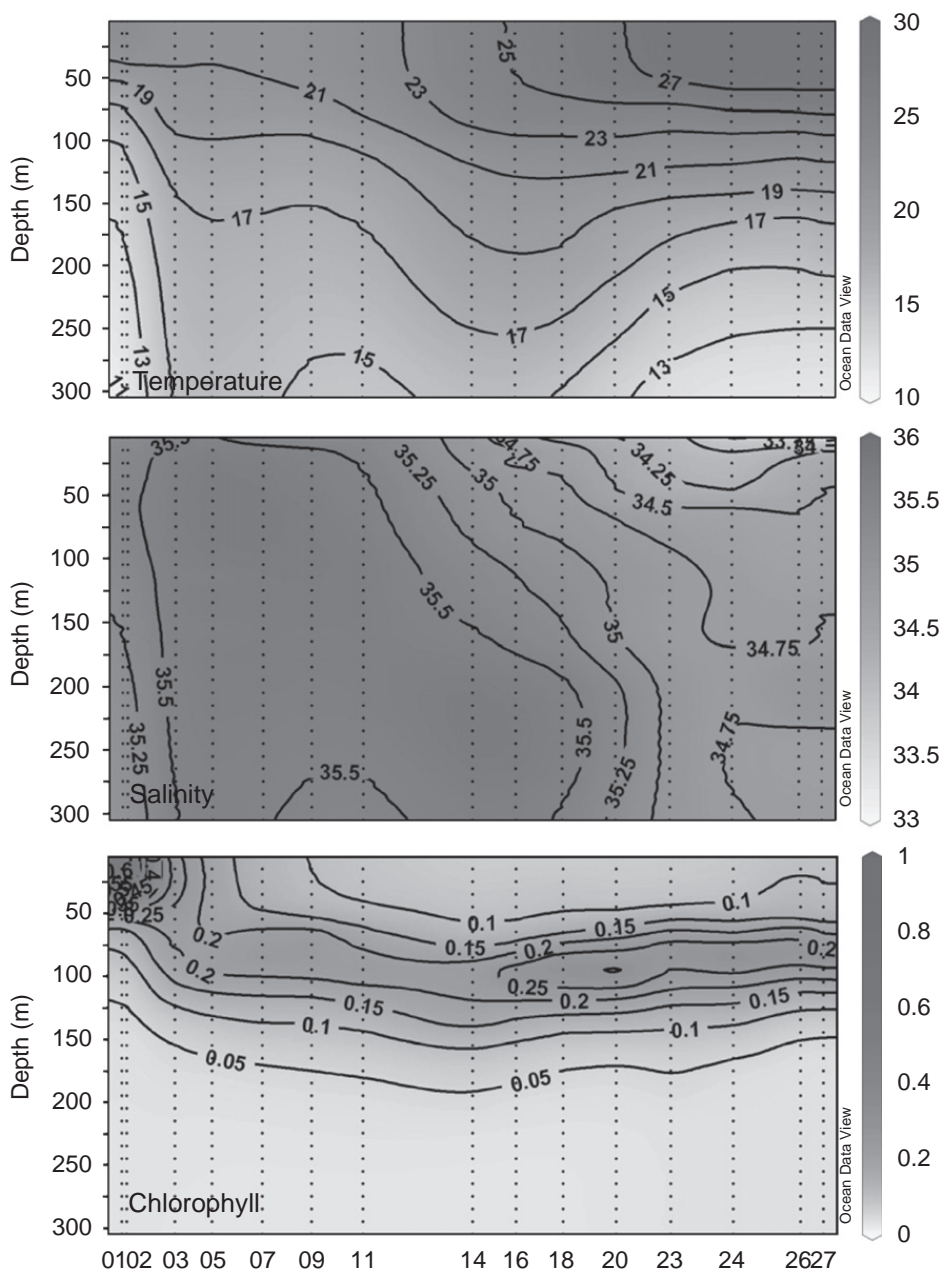


Fig. 2. Depth sections of temperature ($^{\circ}\text{C}$), salinity, and Chlorophyll *a* ($\mu\text{g L}^{-1}$) across the eastward transect from station 01 to 27 (only CTD cast, no discrete water samples were taken at the latter station). The data plotted are based on CTD data binned every 10 m. Depths sections were generated using Ocean Data View software (Schlitzer, 2007).

oceanographic regions can be distinguished across our southwest to northeast transect. The first, south of 30°S and from station 01 to 11, is characterized by relatively low surface temperature ($<23^{\circ}\text{C}$) and homogeneous high salinity throughout the upper water column (35.5) (Fig. 2). Within this region, stations 01–03, closest to the African coast, are influenced by the Agulhas current (AC), while stations 05–11 are located in a zone of recirculation of the ARC (Fig. 1). The second region, including stations 14–27, presents a more stratified water column in terms of both temperature and salinity. Temperatures are high at the surface ($>25^{\circ}\text{C}$) and decrease rapidly below 50 m depth, whereas salinity is lower at the surface (34.25) and increases below 50 m. This second region is primarily influenced by the South Equatorial Current (SEC) and, to a lesser extent, by recirculation from the SIOC (Fig. 1).

Based on chlorophyll data, two distinct regions could also be identified, but their limit (i.e. between stations 03 and 05) differs from those defined by temperature and salinity. Relatively high chlorophyll concentrations were measured at the surface near the African coast (1.3 and $1.1 \mu\text{g L}^{-1}$ at stations 01 and 02, respectively) and decreased sharply below 50 m with no clear DCM (Fig. 2). In contrast, Chl *a* concentrations between stations 05 and 27 were low at the surface ($<0.1 \mu\text{g L}^{-1}$) and showed a deep maximum ($>0.2 \mu\text{g L}^{-1}$) at 75–120 m depth. The DCM was deepest at the very central stations (11–16).

3.2. Inverted microscopy

Except at coastal station 01, where abundances averaged $16,700 \text{ cells L}^{-1}$ for diatoms, $9005 \text{ cells L}^{-1}$ for dinoflagellates, $39,780 \text{ cells L}^{-1}$ for coccolithophorids and $3680 \text{ cells L}^{-1}$ for aloricate ciliates, concentrations of micro- and nanoplanktonic protists in our study were generally low (4068 , 3300 , 3223 , 555 cells L^{-1} on average for diatoms, dinoflagellates, coccolithophorids, and aloricate ciliates, respectively). Comparing abundances of all identified groups (i.e. diatoms, dinoflagellates, coccolithophorids, and ciliates), station 14 in the middle of the transect displayed the lowest concentration with an increase towards the western and eastern portions of the transect (Supplementary Tables 2 and 3). Microplanktonic diatoms were dominated by pennate species throughout the transect (Supplementary Table 2). Diatoms exhibited a clear pattern with highest concentrations in coastal waters, an order of magnitude less in the middle of the

transect and a slight increase again towards Australia. The surface microplanktonic diatom assemblage at the near-coastal stations was dominated by the typical coastal bloom forming species *Pseudo-nitzschia* spp. and *Chaetoceros* subgenus *Hyalochaete* spp. (Supplementary Table 4). The pattern of coccolithophorid abundances resembled that of the diatoms: they were more abundant at station 01, dominated by the bloom-forming species *Emiliania huxleyi* or *Gephyrocapsa oceanica* (coccolithophorids $<10 \mu\text{m}$) (Supplementary Table 4). At open ocean stations, concentrations of coccolithophorids were lower by one order of magnitude and other species dominated the coccolithophorid assemblage (Supplementary Tables 2 and 4). In the other groups (dinoflagellates, aloricate ciliates, nanoplanktonic naked flagellates), the overall gradients described above could also be distinguished but less clearly.

In terms of higher level taxonomic groups, concentrations of diatoms, coccolithophorids, dinoflagellates, and ciliates showed no clear differences between surface and DCM. The only exception was micro- and nanoplanktonic diatoms at station 01, where concentrations at surface were much higher than at depth (Supplementary Table 2). In contrast, different species, or genera, of both microplanktonic diatoms and large ($>10 \mu\text{m}$) and small ($<10 \mu\text{m}$) coccolithophorids, dominated the surface and DCM assemblages at all stations (Supplementary Table 4). Microplanktonic dinoflagellate assemblages were always dominated by *Gymnodinium* and *Gyrodinium* spp. The inverted microscopy method precluded determination of species within these genera, and possible differences at that level could not be detected. The same holds true for aloricate ciliates.

3.3. Epifluorescence counts

Microscopic counts of small phototrophic and heterotrophic protists (PP and HP, respectively) were performed at several depths from selected stations (Table 1). Station 01 stood apart because it had no clear DCM and the highest PP numbers were observed at the surface ($14 \times 10^3 \text{ cells mL}^{-1}$). Therefore, it was not included in the computation of average values shown in Table 2 for three water layers: samples above (i.e. surface), at the DCM, and below the DCM (down to 200 m depth). As for HP (range $0.3\text{--}0.7 \times 10^3 \text{ cells mL}^{-1}$), PP abundances were remarkably constant (range $1\text{--}4 \times 10^3 \text{ cells mL}^{-1}$) both above and at the DCM. The higher variability observed for PP below the

Table 2

Cell counts (cell mL^{-1}) and size fractionation of small protists (typically flagellated) under epifluorescence microscopy after DAPI staining

	Phototrophic protist (PP)					Heterotrophic protist (HP)					% Protists	
	Mean	Range	Size fractions (%)			Mean	Range	Size fractions (%)			PP	HP
			2–3 μm	4–5 μm	> 5 μm			2–3 μm	4–5 μm	> 5 μm		
Surface	1140	560–1820	90	9	1	480	250–740	86	10	4	70	30
DCM	2930	1160–4620	94	5	1	400	280–490	85	12	3	87	13
Below DCM	630	40–1580	96	3	1	200	70–340	82	14	4	60	40

DCM was due to the heterogeneity of the samples considered (i.e. greater depth range, light and nutrient gradients). PP numbers were highest at the DCM, lowest below, and intermediate at the surface. In contrast, HP reached highest abundance at the surface and showed less variability than PP across the depth profiles. PP cells were always more abundant than HP, but their ratio varied significantly among the three water layers, being highest at the DCM and lowest below (Table 2). Epifluorescence counts also allowed an approximate estimate of the size structure of the protist community. These data showed

constant trends with 85–95% of the cells in the size range of 2–3 μm , and very few cells larger than 5 μm (Table 2). This larger size fraction is better estimated by inverted microscopy (Supplementary Table 3).

3.4. Flow cytometry

Eukaryotes, *Prochlorococcus*, and *Synechococcus* were enumerated by flow cytometry across the transect (Fig. 3). Data shown correspond to non-fractionated seawater

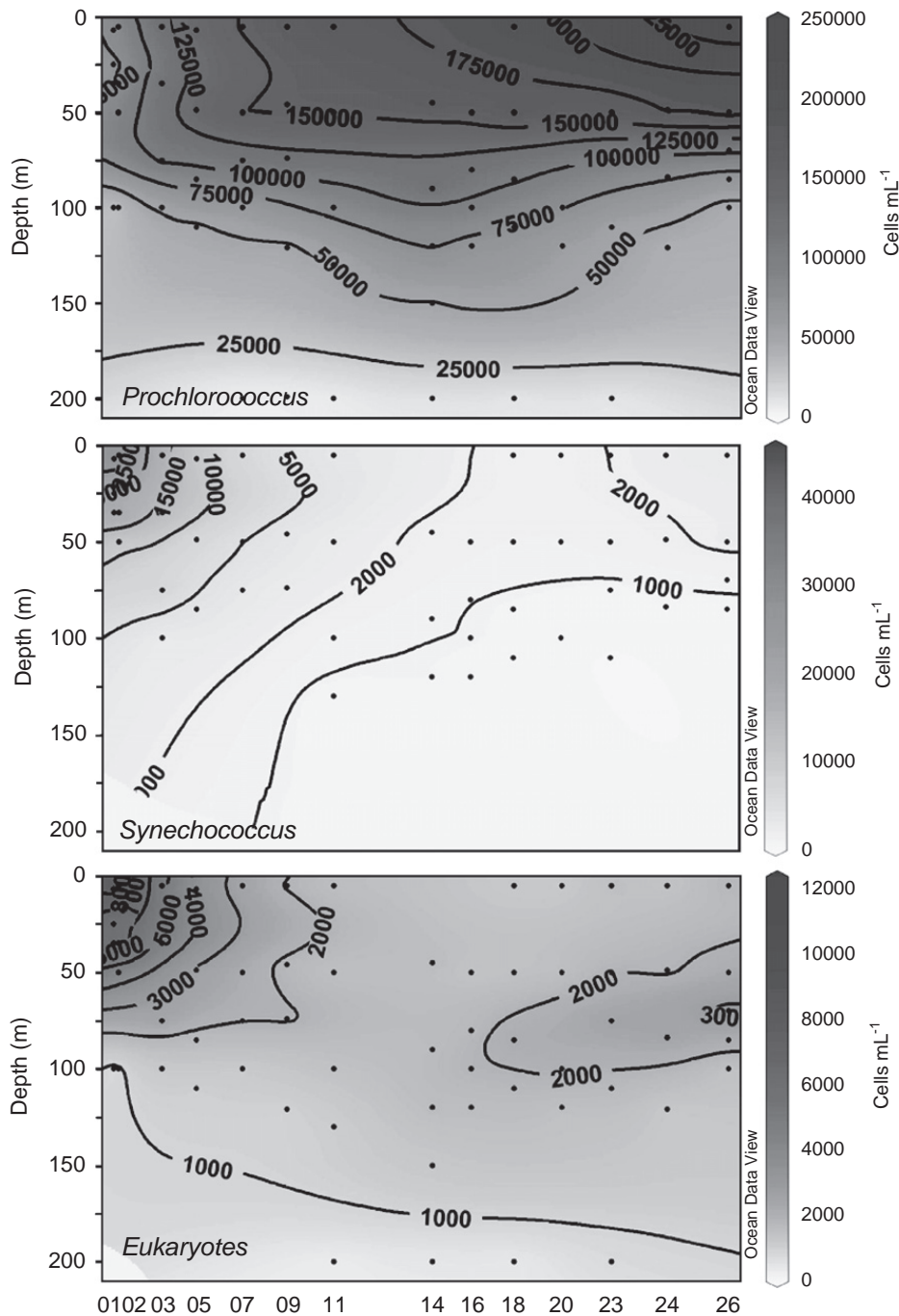


Fig. 3. Depth sections for cell densities of *Prochlorococcus*, *Synechococcus*, and eukaryotes (cells mL^{-1}), from the total size fraction, assessed by flow cytometry across the eastward transect. Black dots correspond to actual sampling depths. Depth sections were generated using Ocean Data View software (Schlitzer, 2007).

samples. Counts from 3 μm pre-filtered samples yielded very similar numerical values and distributional patterns, indicating that most cells inspected by flow cytometry were smaller than 3 μm . Indeed, chlorophyll-containing eukaryotes, *Synechococcus*, and *Prochlorococcus* in the <3 μm size fraction accounted for 92%, 96%, and 102% of cells from the total size fraction, respectively (data not shown). In addition, very good correlations were found between counts obtained by epifluorescence microscopy and the more extensive dataset analyzed by flow cytometry, both for phototrophic eukaryotes ($n = 32$, $y = 0.9549x + 293$, $R^2 = 0.94$) and *Synechococcus* ($n = 23$, $y = 0.9638x + 528$, $R^2 = 0.99$).

The first three stations were characterized by high abundances of phototrophic picoeukaryotes ($> 1 \times 10^4$ cells mL^{-1} at surface) and *Synechococcus* (up to 4.7×10^4 cells mL^{-1}) (Fig. 3). Between stations 05 and 11 we observed a continuous increase in *Prochlorococcus* cell densities (up to 2×10^5 cells mL^{-1}) concomitant with a decrease of *Synechococcus* (down to less than 3×10^3 cells mL^{-1}) (Fig. 3). Picoeukaryotic cell densities also decreased (down to 10^3 cells mL^{-1}) from the African coast towards the subtropical gyre, and their maximal densities dropped from the surface to the DCM. In oligotrophic areas, *Prochlorococcus* reached maximum concentrations within the top 50 m of the water column ($> 1.5 \times 10^5$ cells mL^{-1}) and decreased sharply to abundances below 7.5×10^4 cells mL^{-1} between 50 and 100 m depth. *Synechococcus* were very scarce in this region, although a slightly higher abundance was noted at station 26. Picoeukaryotes were in low abundance at the surface and maintained constant maximal densities (ca. 1.5×10^3 cells mL^{-1}) at depths between 75 and 125 m. We observed a moderate increase in cell numbers together with slightly less deep maxima at the eastern-most stations (23, 24, and 26) (Fig. 3).

3.5. Denaturing gel gradient electrophoresis

Spatial variability of the picoeukaryotic assemblages was analyzed by the fingerprinting technique DGGE of the 18S rRNA gene (Fig. 4). Changes in diversity along the transect were studied in separate gels for surface and DCM samples (Fig. 4A). In both cases, there was a gradual change in diversity along the transect, with the dominant shift in the middle of the transect, between stations 9 and 11 at surface and between 11 and 14 at DCM. The general trend shows that picoeukaryotic assemblages were relatively uniform in vast areas of the Indian Ocean at the same depth. Indeed, many DGGE bands were found in most open sea samples, indicating picoeukaryotic populations with large oceanographic distributions. In contrast, higher variability was observed between the two depths analyzed. This was clearly shown in a dendrogram combining both gels (Fig. 4A, right panel), using only the 14 bands (out of 32 bands at the surface gel and 36 bands at the DCM gel) that could be unambiguously assigned in both gels. These 14 bands were also the most intense, accounting for 80% of band intensity on average. The dendrogram showed a main separation in the middle

of the transect and, remarkably, all surface samples from stations 9 to 24 in one cluster and all DCM samples from stations 14 to 24 in another cluster. Therefore, picoeukaryotic assemblages appeared more similar among surface (and DCM) samples ~5000 km apart (stations 14–24) than between surface and DCM samples at each station. This indicates a clear distinction of surface and DCM waters in terms of picoeukaryotic community composition.

In order to study changes along the vertical profile in greater detail, we completed additional DGGE analyses with six depth samples at four selected stations along the transect (Fig. 4B). At all stations investigated there was a clear shift in the picoeukaryotic assemblages across the water column. Although some DGGE bands were found across the depth profile, samples above the DCM were similar. Nevertheless, one can notice the gradual shift among the surface, the DCM and deeper samples. This emphasizes the importance of the vertical gradient in picoeukaryotic diversity with a clear distinction of surface, DCM, and mesopelagic waters.

3.6. 18S clone libraries

Based on the DGGE analysis, we selected eight samples (stations 01, 09, 18, and 23, at two depths: surface and DCM located at 25, 74, 85, and 75 m, respectively) to prepare clone libraries of the 18S rRNA genes representative of protists smaller than 3 μm . The two libraries from station 01 yielded few clones and are presented together. In fact, as previously mentioned, station 01 did not have a clear DCM and both samples (surface and 25 m) were characterized by very similar DGGE fingerprints. Between 52 and 139 sequences were analyzed for each of the seven libraries (541 sequences in total). A Blast analysis of these sequences (Supplementary Table 5) revealed that six phylogenetic groups accounted for 75% of the total sequences in all libraries: dinoflagellates, marine alveolates I and II, marine stramenopiles (MASTs), prasino-phytes, and radiolarians (Fig. 5A). These sequences were highly related to environmental sequences retrieved in other oceans, including the Pacific, the Atlantic, and the Arctic and Mediterranean Seas. The average similarity with the closest Blast sequence match within these six groups was 98.7%, 99.1%, 97.0%, 98.6%, 99.6%, and 97.2%, respectively. Marine alveolate II and radiolarian sequences from the Indian Ocean are slightly more distinct from already known sequences than the other taxonomic groups. The coastal library was unique in having an important contribution of prasinophyte sequences. As previously observed in the DGGE analysis, the phylogenetic diversity of the taxa detected (at the level of major groups) was rather similar among the open ocean samples from the same depth layer, whereas surface and DCM samples were more different (Fig. 5A). Most apparent were the higher contribution of radiolarian and prasinophyte sequences and the lower contribution of marine alveolates I in the DCM libraries.

Up to 25% of sequences from each library did not belong to any of these six major groups and their

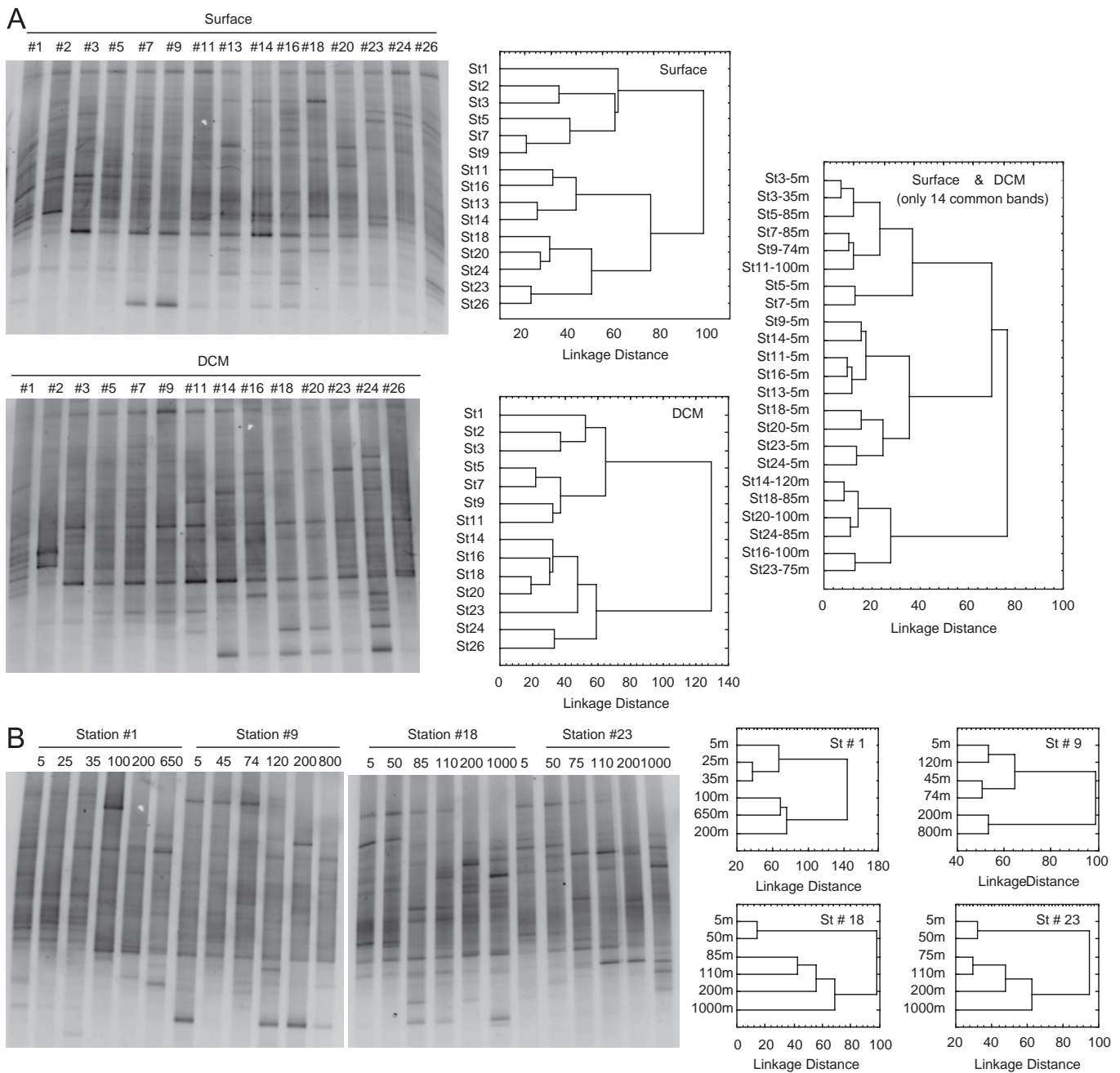


Fig. 4. Comparison of the diversity of picoeukaryotic assemblages by DGGE fingerprints and cluster analysis. (A) Surface and DCM samples along the entire transect: DGGE gels (left), dendrograms from the gels (middle), and the dendrogram combining both gels using only 14 common bands unambiguously assigned (right). (B) Depth profiles at selected stations: DGGE gels (left) and dendrograms for each station (right).

affiliation is shown together for all libraries (Fig. 5B). These less well-represented groups accounted for a significant fraction of the genetic diversity in the clone libraries analyzed. Chrysophytes, bicosoecids, ciliates, and apusozoans yielded more than 10 sequences, whereas other well-known marine groups are represented by a smaller number of clones. Notable is the relatively high number of sequences (22) with uncertain affinities to any particular group, not even to a main eukaryotic supergroup, using Blast search. Complete sequencing of these clones, together with extensive and careful phylogenetic analysis, would be necessary to achieve a better estimate of their putative phylogenetic affiliation.

3.7. Pigment analysis

Phytoplankton pigments were measured by HPLC on surface and DCM samples for three size fractions: total, >3 μm, and <3 μm. Total Chl *a* in the surface was much higher at stations 01–03 than for the rest of the transect (Fig. 6), where concentrations remained around 0.120 μg L⁻¹ (±0.045 S.D.). As expected, the pigment composition of the largest size fraction (>3 μm) could be attributed almost exclusively to eukaryotes (96%). On average, the pico-size fraction (<3 μm) contributed to 89% of the total Chl *a* (88% at surface and 90% at DCM), highlighting the importance of the smallest size fraction of primary

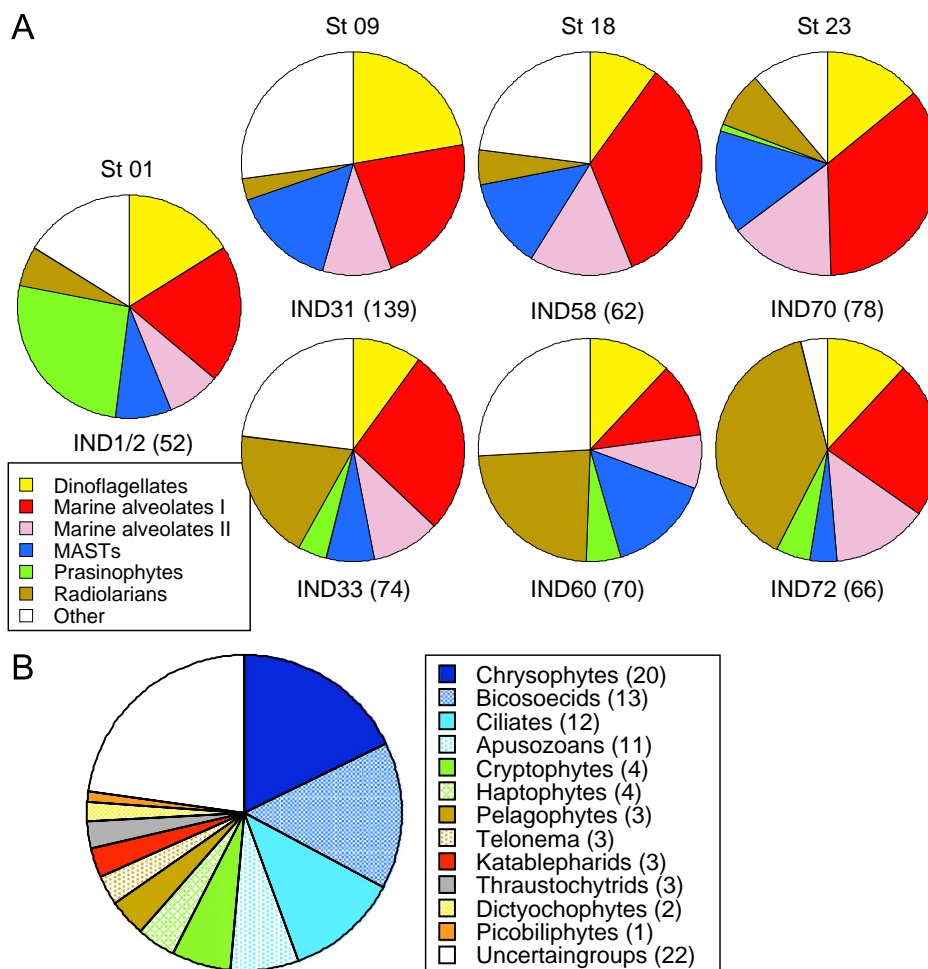


Fig. 5. Taxonomic affiliation of sequences retrieved in 18S rDNA clone libraries from stations 01, 09, 18, and 23 at the surface (libraries IND1, IND31, IND58, and IND70, respectively) and DCM (libraries IND2, IND33, IND60, and IND72, respectively). (A) Clonal contribution of the six most represented taxonomic groups (the two libraries for station 01 are presented together). The number of sequences analyzed in each library is indicated after the library name. (B) The contribution of less well represented groups in the eight libraries combined. The number of sequences found in each taxonomic group is indicated.

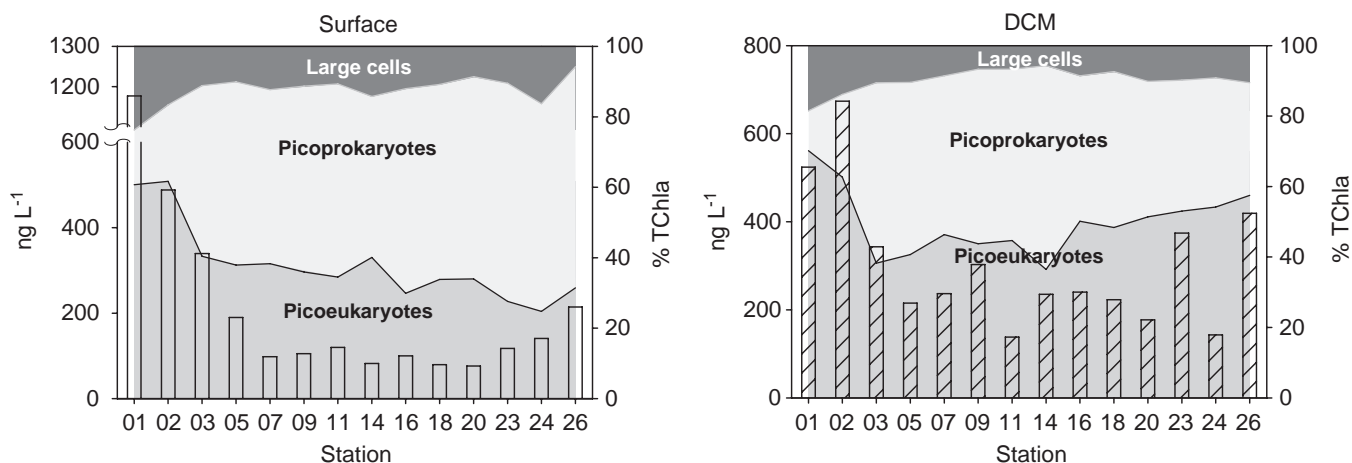


Fig. 6. Contribution of picoprokaryotes (*Synechococcus* and *Prochlorococcus*), picoeukaryotes, and large (>3 μm) phytoplankton cells to the total Chl *a* along the transect in Surface and at the DCM (25 m depth for station 01). Chl *a* in phytoplankton larger and smaller than 3 μm was obtained from size fractionation. The contribution of *Synechococcus* and *Prochlorococcus* to the small fraction was estimated from the adsorption of the Chl *a* to the different groups using Chemtax (see text for details). Bars represent absolute Chl *a* concentration for each station.

producers along the transect. The picophytoplankton contribution was comparable in coastal (84% on average for stations 01–03) and oceanic (90% on average for stations 05–26) environments (Fig. 6). At the surface,

picoeukaryotes contributed 38% to the total Chl *a*, 54% at stations 01–03 and 33% at stations 05–26. At the DCM, this contribution increased to 50% on average, being 57% at stations 01–03 and 48% at stations 05–26.

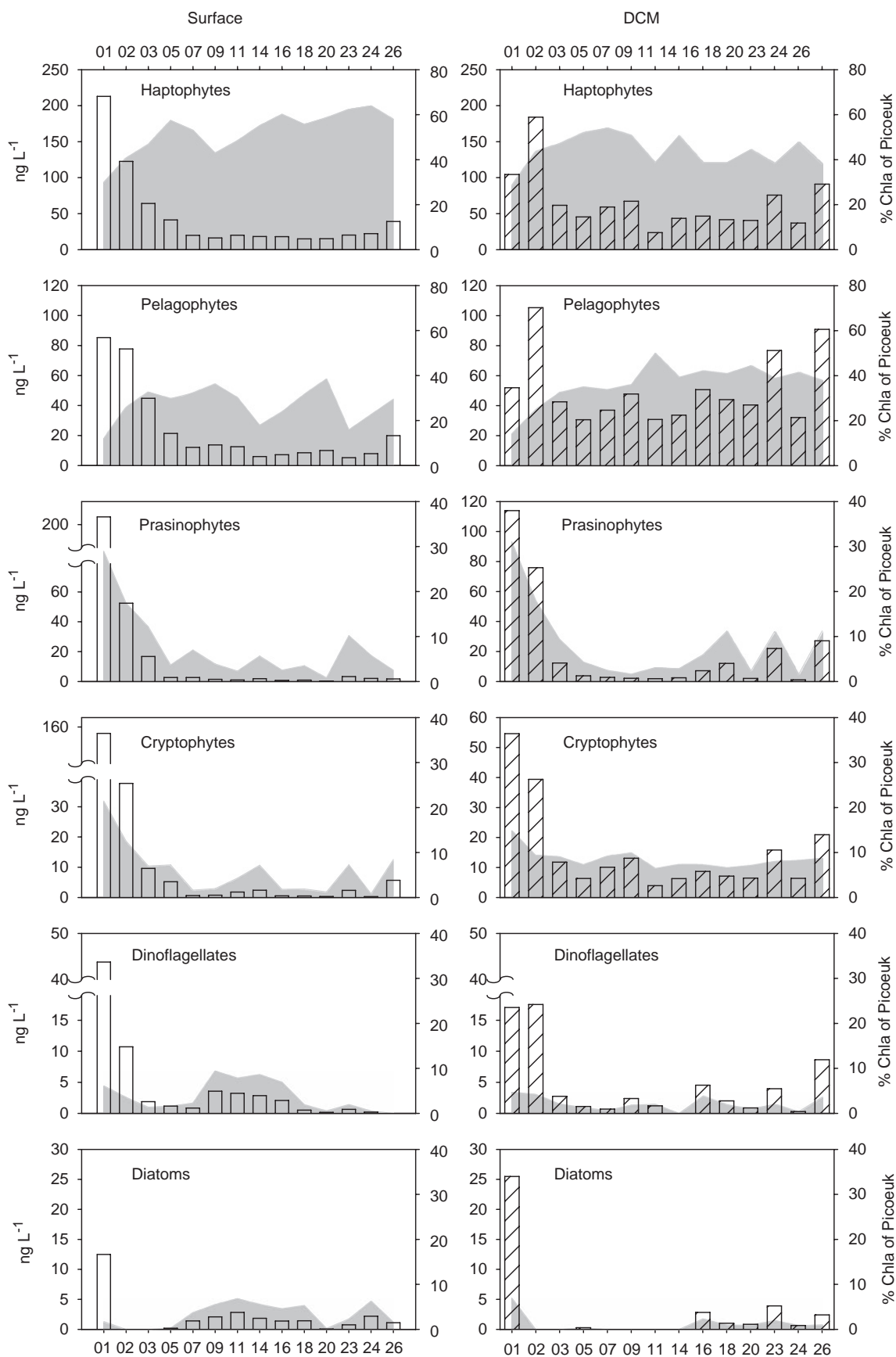


Fig. 7. Distribution of total Chl *a* among eukaryotic picoplankton of six phytoplankton groups, as distinguished by their pigment suites. Bars represent absolute Chl *a* concentration attributed to each picoeukaryotic group after Chemtax (see text for details) and the shadowed areas their relative contribution to total picoeukaryotic Chl *a*.

Using Chemtax we investigated the relative contributions of six major eukaryotic chemotaxonomic groups (haptophytes, pelagophytes, prasinophytes, cryptophytes, dinoflagellates, and diatoms) to Chl *a* in the three size fractions (Fig. 7). Because of the strong dominance of the pico-size fraction in pigment biomass, results obtained for the total fraction matched the pattern observed in smaller cells. Actual values of characteristic pigments (ng L^{-1}) for each taxonomic group considered for the total size fractions is presented in Supplementary Table 6. At both depths and all stations across the transect, haptophytes and pelagophytes were clearly the dominant eukaryotic pigment groups (Fig. 7). Prasinophytes made a significant contribution ($\sim 20\%$ of the picoeukaryotic fraction of Chl *a*) at the more eutrophic coastal stations 01–03, decreasing to 5% in the more oligotrophic open sea stations. Cryptophytes also displayed a similar pattern but their contribution was lower than that of the prasinophytes (6% at surface and 9% at DCM). As expected, the contribution of dinoflagellates and diatoms was low in the picoplanktonic fraction because of the typically large size of these organisms. However, within the pico-size fraction, one can notice their higher contribution in surface in the central part of the transect. Overall, these two groups were present mostly in the large size fraction near the African coast, where they contributed up to 15% of total Chl *a*. According to their pigment signature, samples

clustered according to depth rather than to location especially for the most oceanic stations 07–24 (Fig. 8)

3.8. Fluorescent *in situ* hybridization

The distribution of protists detected by general eukaryotic probes matched the distribution obtained from flow cytometry (Figs. 3 and 9A). Cells detected by the chlorophytes probe were more abundant at coastal stations, where they always reached abundances in excess of 2000 cells mL^{-1} and up to 8900 cells mL^{-1} in the photic zone of stations 01–03, and contributed up to 51% of total picoeukaryotes detected by FISH at these stations (70% at surface) (Supplementary Table 7, Fig. 9A). In the oceanic region (stations 05–18), chlorophyte densities were much lower (typically < 500 cells mL^{-1}) and contributed on average to 19% of total picoeukaryotes (10% at the surface and 24% at the DCM) (Fig. 9A and Table 3). Along the transect, haptophytes were most abundant in the upper water column, in particular above 75 m (Fig. 9A). Although their abundance decreased from the coast to the gyre, they always contributed a significant portion of the picoeukaryotic community of the upper water column in oligotrophic areas (14% at the surface, up to 36% at 45 m depth at station 09). In contrast, their contribution was lower at the DCM (on average 8% of picoeukaryotic cells, Table 3).

Within the chlorophyte division, we estimated the contribution of three Mamiellales (prasinophytes) genera, namely *Micromonas*, *Bathycoccus*, and *Ostreococcus*. As for chlorophytes, and more generally for total picoeukaryotes, we observed high abundance of the genus *Micromonas* at coastal stations (> 750 cells mL^{-1} , 19% of total picoeukaryotes at station 01, surface). As waters became more oligotrophic, a rapid decrease in abundance was observed with maxima always below 100 cells mL^{-1} at all depths in the gyre (Fig. 9B). The genus *Bathycoccus* was characterized by lower abundance (max 200 cells mL^{-1}), but displayed a spatial pattern similar to that of *Micromonas* along the transect (Fig. 9B). At coastal stations, maximum abundances for *Bathycoccus* were observed at slightly lower depths than for *Micromonas* (Fig. 9B). Finally, the genus *Ostreococcus* was always found at low densities (< 100 cells mL^{-1}). Maximal densities of *Ostreococcus* deepened towards oligotrophic waters following the DCM trend (Fig. 9B).

4. Discussion

4.1. Picoplankton contribution to phytoplankton biomass and its distribution

The analysis of size fractionated samples with different techniques showed that photosynthetic cells from the pico-size fraction were numerically dominant and had the highest contribution to Chl *a* biomass throughout the transect (Figs. 3 and 6 and Table 2). This observation agrees with most studies that performed size fractionated analyses in various open ocean ecosystems. For instance, in a study including temperate, subtropical, equatorial and

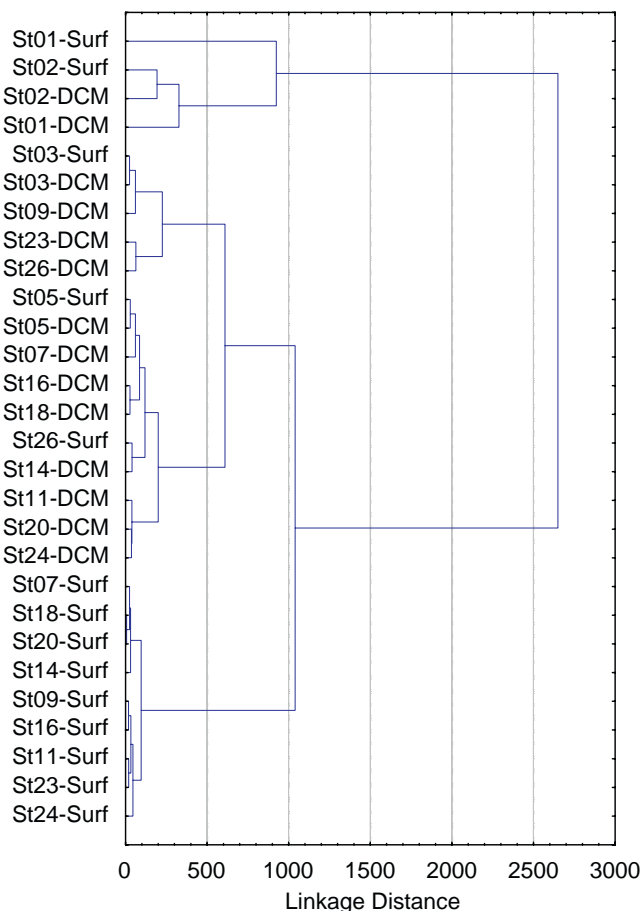


Fig. 8. Clustering of samples according to their pigment signatures. Pigments and procedures applied are described in Section 2.

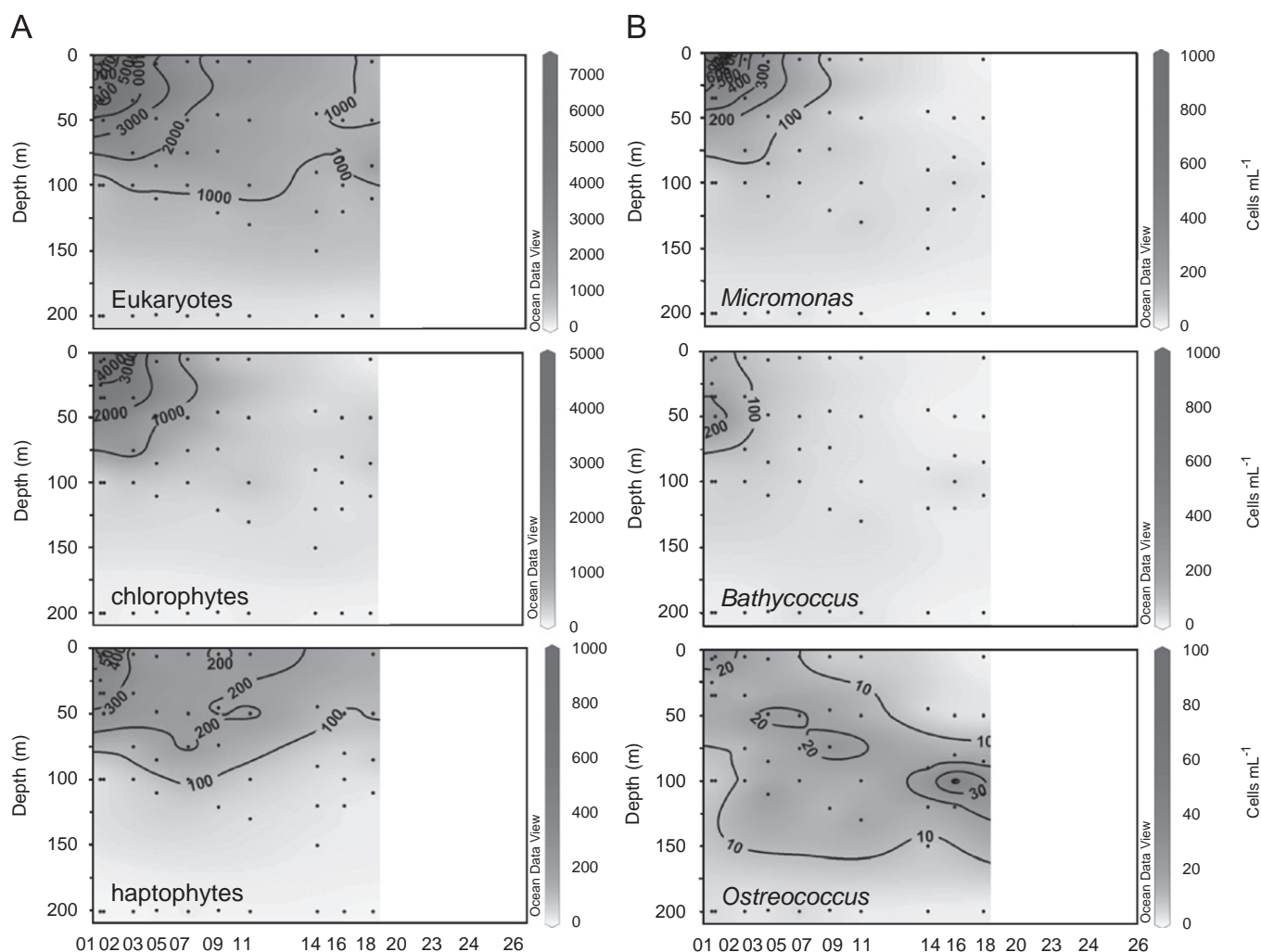


Fig. 9. Depth sections of picoeukaryote densities (cells mL⁻¹) estimated by TSA-FISH along the transect (stations 01–18). (A) All picoeukaryotes targeted by a mix of eukaryotic probes (top), cells targeted by the chlorophyte-specific probe (middle), and cells targeted by the haptophyte-specific probe (bottom). (B) Cell density estimates for the *Micromonas* (top), *Bathycoccus* (middle), and *Ostreococcus* (bottom) genera (chlorophytes, prasinophytes, Mamiellales). Black dots correspond to samples. Depth sections were generated using Ocean Data View software (Schlitzer, 2007).

Table 3
Average contribution (%) of taxonomic groups across the transect performed and according to the technique used

	01–03 surface			05–26 surface			05–26 DCM		
	HPLC	Clone libraries	FISH	HPLC	Clone libraries	FISH	HPLC	Clone libraries	FISH
Haptophytes	39	0	4	56	2	14	45	0	8
Chlorophytes/prasinophytes	20	26	70	4	0	10	5	5	24
Pelagophytes	23	0	–	28	0	–	40	2	–
Dinoflagellates	4	16	–	4	15	–	2	11	–
Diatoms	1	0	–	4	0	–	1	0	–
Cryptophytes	15	6	–	4	0	–	8	0	–
Marine alveolates	–	28	–	–	44	–	–	31	–
Radiolarians	–	6	–	–	5	–	–	27	–
MASTs	–	8	–	–	14	–	–	9	–
Chrysophytes	–	4	–	–	4	–	–	2	–
Ciliophora	–	4	–	–	2	–	–	1	–
Other phototrophs	–	0	–	–	1	–	–	0	–
Other heterotrophs	–	2	–	–	7	–	–	6	–
Undetermined groups	0	0	26	0	4	76	0	6	68

Estimates obtained by HPLC correspond to the contribution to picoeukaryotic Chl *a*. Values for clone libraries are contribution to total number of sequences encountered in the picoplankton size fraction. Data for FISH are contribution to total picoeukaryotes cells enumerated by FISH (picoplankton size fraction). (–) Averaged data not available.

upwelling environments, picoplankton contributed most to total Chl *a* (Marañón et al., 2001). This was particularly true for equatorial and subtropical waters in which picoplanktonic organisms accounted for 80% of total Chl *a*, and 60–70% of primary productivity (Marañón et al., 2001). Another study presenting data from a cruise conducted in the Arabian Sea in the inter-monsoon period (March–April 1995) indicated that 85% of total Chl *a* passed through a 2 µm filter (Latasa and Bidigare, 1998). Our values are somewhat higher (around 90%), likely because we performed the size-fractionation through 3 µm instead of 2 µm.

The patterns of abundance and distribution observed for the two cyanobacterial genera and for picoeukaryotes from flow cytometry and pigment analyses are in agreement with previous data. *Prochlorococcus* was dominant in oligotrophic areas, while picoeukaryotes and *Synechococcus* usually co-varied and contributed a higher proportion at the more “coastal”, nutrient-rich stations (Zubkov et al., 1998; Worden and Not, 2008). Recent observations made along longitudinal cruise tracks passing through large ecological provinces such as the Pacific Equatorial Divergence Province (PEQD) and the South Pacific Subtropical Gyre Province (SPSG) showed little variation with respect to the contribution of these three picoplanktonic components within the same province (Dandonneau et al., 2006), as reported here. In contrast, latitudinal ocean basin scale cruises such as the Atlantic Meridional Transects (AMT), which passed through several contrasting ecological provinces, identified more pronounced variations in the picoplankton community structures (Zubkov et al., 1998; Marañón et al., 2001).

Picoeukaryotes contribute significantly to global primary productivity (Li, 1994; Worden et al., 2004). Surprisingly, the composition of picoeukaryotic assemblages can be remarkably constant over broad oceanographic regions (Díez et al., 2004). Indeed our data show that, on the horizontal scale, picoeukaryotes from the Indian Ocean consist of two distinct major assemblages containing members of a variety of phylogenetic groups. Results from the various techniques applied (e.g. clone libraries, HPLC, FISH) show that the most striking differences in biomass and community composition occurred between the first three stations and the oceanic stations. These regions correspond to two of the ecological provinces defined by Longhurst (1998), namely the Eastern Africa Coastal (EAFR) province and the Indian South Subtropical Gyre (ISSG) province. Considering the latter, apparently, homogeneous province, one can observe greater variation in the picoeukaryote assemblages vertically in the upper 200 m of the water column than horizontally across the whole transect (ca. 10,000 km). This is particularly notable in results from the clone libraries (Fig. 5), pigment analyses (Fig. 8), and DGGE fingerprinting (Figs. 4B).

4.2. Diversity and distribution of major picoeukaryotic taxa

Despite the occurrence of general patterns in the community composition and distribution, such as the

important contribution of prasinophytes in coastal environments, and of haptophytes and pelagophytes in the open ocean (Table 3), important discrepancies were observed between techniques for particular taxonomic groups.

4.2.1. Haptophytes

Our pigment analyses suggested that haptophytes were important throughout the transect and particularly in oligotrophic waters (Fig. 7), in agreement with previous work (Ondrusek et al., 1991; Bidigare and Ondrusek, 1996). For example, in the equatorial Pacific, haptophytes contributed 30–40% of Chl *a* biomass in the upper 100 m of the water column (Mackey et al., 1998). At station ALOHA, off Hawaii, haptophytes contribute 22% of total Chl *a* biomass at the DCM (Letelier et al., 1993). In a study examining haptophytes by electronic microscopy, haptophyte contributions to total abundance of photosynthetic eukaryotes were in the same range, from 10% to 50%, along a vertical profile (Andersen et al., 1996). In contrast, our clone libraries recovered only a few haptophytes sequences (Fig. 5) in agreement with the molecular data of Moon-van der Staay et al. (2000) in the Equatorial Pacific. Higher GC content of the 18S rDNA gene in haptophytes may prevent consistent PCR amplification (C. de Vargas, personal communication). Similarly, the contribution of haptophyte cells observed by FISH was lower than from pigment analysis (Table 3). These discrepancies could be due to the fact that the cellular concentration of pigments varies according to environmental parameters and physiological status (Falkowski and LaRoche, 1991; Mackey et al., 1998) or that haptophyte cells may be slightly larger than other picoeukaryotes (e.g. prasinophytes, see Fig. 6 in Not et al., 2005) and therefore have higher pigment content.

4.2.2. Chlorophytes and prasinophytes

Cells belonging to the chlorophyte division represented 70% of the cells detected by FISH in surface waters of stations 01–03. Accordingly, prasinophytes were very important at coastal stations, and were observed to contribute ~20% of picoeukaryotic Chl *a* in pigment analysis of surface waters (29% in surface water at station 01). All techniques suggested a contribution decreasing from the EAFR province towards the ISSG province (Table 3). The lower abundance of prasinophytes in the open ocean as compared to coastal waters has been previously observed in studies using pigment analysis (Letelier et al., 1993; Andersen et al., 1996; Carreto et al., 2003), electron microscopy (Thomsen and Buck, 1998), and FISH (Not et al., 2005). With respect to vertical distribution in the ISSG province, pigment analysis showed a rather constant contribution between surface and DCM samples, while both FISH and clone libraries found more green algae at the DCM (Table 3).

The pattern observed for *Micromonas* (Fig. 9B) matched that observed for chlorophytes (on average *Micromonas* accounted for 28% of chlorophytes cells), confirming the ubiquity and significant contribution of this genus as a key eukaryotic species in some marine ecosystems (Thronsen, 1976; Thomsen and Buck, 1998; Not et al., 2005). However,

the average contribution of *Micromonas* to picoeucaryotes is markedly lower than at very coastal sites, such as in the English Channel off Roscoff, where it represented on average 45% of picoeukaryotic cells throughout the year (Not et al., 2004). Although present in low abundance in the Indian Ocean, *Ostreococcus* maintained a constant maximal cell density at depth, which deepened with the DCM. The observed distribution may be partially explained by the presence of *Ostreococcus* strains adapted to low light level (Rodríguez et al., 2005).

4.2.3. Pelagophytes and chrysophytes

Our results for pelagophytes were somewhat similar to those of the haptophytes: pigment signatures indicated high abundance (Fig. 7) but very few sequences were retrieved in clone libraries from the corresponding samples. Pelagophytes were initially isolated from the pelagic environment (Andersen et al., 1993), and since then have been described as significant components of pelagic ecosystems based on pigment studies (Bidigare and Ondrusek, 1996; Latasa et al., 1997; Suzuki et al., 1997; DiTullio et al., 2003). However, one should note a certain confusion when dealing with chrysophytes and pelagophytes, as some of the researchers working with pigment signatures use the term chrysophyte *sensu lato* to refer to organisms presenting 19'-butanoyloxyfucoxanthin, a pigment typically ascribed to pelagophytes (Mackey et al., 1996; Wright and Jeffrey, 2006). The lack of photosynthetic marine chrysophytes in culture prevents characterization of their pigment signature and, consequently, proper discrimination from pelagophytes and diatoms. In contrast to the few pelagophyte sequences retrieved in the Indian Ocean clone libraries, we found a significant number of chrysophyte sequences. Most of these form novel lineages (Supplementary Table 5) of uncertain trophic mode (i.e. photosynthetic or heterotrophic). Chrysophyte sequences have also been observed in recent surveys (Fuller et al., 2006a; Worden and Not, 2008), suggesting a significant role for this group in pelagic ecosystems. The actual contribution of pelagophytes and chrysophytes to picoeukaryotic communities in the open ocean could be resolved by FISH techniques, but reliable probes are not yet available for these groups.

4.2.4. Other phytoplanktonic groups

We observed a significant pigment contribution of cryptophytes within the pico-size fraction, especially at the DCM throughout the transect. A few small cryptophytes (around $4 \times 6 \mu\text{m}$ in size) were seen under epifluorescence microscopy, accounting for up to 1–3% of phototrophic cells. Their larger size (but likely passing through the $3 \mu\text{m}$ filter because of their oblong shape) could explain in part their larger contribution using pigment analysis against microscopic counts. The few cryptophyte sequences in our clone libraries all came from the first stations (Table 3); thus, the precise taxonomic affiliation of these open ocean cryptophytes remains unresolved.

According to inverted microscopic observations, diatoms and dinoflagellates were dominated by cells smaller than $20 \mu\text{m}$ but bigger than $3 \mu\text{m}$ (Supplementary Tables 2

and 3). The pigment signature for both groups was observed in most picoplanktonic samples and their contribution to picoeukaryotic Chl *a* was higher in the gyre. Diatom pigments could have come from bolidophytes or small pennates, which could have passed through a $3 \mu\text{m}$ filter along their smallest dimension and would be more abundant in the gyre than in the more coastal domain. Alternatively, cell breakage during pre-filtration is possible for both diatoms and dinoflagellates. In contrast to pigment analyses, clone libraries retrieved neither diatom nor bolidophyte sequences but a large number of dinoflagellate sequences (10–20% of sequences retrieved). However, as is observed for a significant fraction of the micro-nano-plankton (Sherr and Sherr, 2000), we cannot exclude that the dinoflagellates from the pico-size fraction are heterotrophic, which would prevent detection using pigment techniques.

4.2.5. Non-photosynthetic organisms

In our study, a significant proportion of sequences (at least 25%) from each library affiliated to marine alveolates (potentially mostly parasites; Groisillier et al., 2006; Dolven et al., 2007) and MAST (being largely free-living bacterivorous flagellates; Massana et al., 2006). These sequences are closely related (more than 97% similarity) to environmental sequences retrieved in other oceans, including Pacific (Moon-van der Staay et al., 2001), Atlantic (Not et al., 2007), Arctic (Lovejoy et al., 2006), and Antarctic (López García et al., 2001), confirming the cosmopolitan distribution of these taxa.

In the Indian Ocean, radiolarian sequences were particularly abundant in DCM libraries (Fig. 5A). In oceanic samples, the radiolarians (typically microplanktonic protists) were well represented in clone libraries from the pico-size fraction, and mainly observed at the DCM (Yuan et al., 2004; Marie et al., 2006), or even at greater depths (Countway et al., 2007; Not et al., 2007). The actual size and ecological function of the organisms linked to these sequences remain currently unresolved (see Not et al., 2007 for discussion).

4.3. Methodological considerations and further investigations

The multi-technique approach allowed overall trends to be established, despite the limitations of each technique (Table 3). For example, the current pigment ratios used in Chemtax are probably well adapted for micro- and nano-phytoplankton but may need some fine-tuning when examining picoplankton for which cultures are still often lacking. Moreover, the characterization of minor pigments should be developed in order to increase the discrimination among phytoplankton groups (Latasa et al., 2004).

A notable bias towards specific protist groups, in particular heterotrophic ones, is regularly observed in clone library genetic surveys (Vaulot et al., 2002, Table 3). Part of the explanation could come from the significant variation in the copy number of the 18S rRNA gene between different taxa (Zhu et al., 2005), such that

organisms with more copies are more readily detected following PCR. Other factors influencing DNA accessibility (e.g. the toughness of the cell membrane) might account for the differences observed between auto- and heterotrophic organisms as well. Strategies currently developed to target more specifically photosynthetic picoeukaryote diversity include building clone libraries from flow cytometrically sorted populations (Shi and Marie, personal communication), targeting plastid genes (Fuller et al., 2006a), or using taxon-specific sets of primers (Viprey et al., 2008). Moreover, clone libraries based on environmental rRNA instead of DNA could give access to the actively growing part of assemblages (Stoeck et al., 2007).

In the present work, 70% of cells could not be identified by the chlorophyte and haptophyte FISH probes used. This highlights the need to develop a more comprehensive set of probes. Moreover, since FISH counts provide absolute cell abundance together with some estimation of cell size and shape, this approach would be helpful in obtaining information for groups such as radiolarians, pelagophytes, chrysophytes, or marine alveolates. Finally, quantitative PCR would be valuable to establish large-scale trends along with fine spatial resolution of particular species or ecotypes (Johnson et al., 2006), allowing us to understand much better their distribution along horizontal and vertical gradients.

Acknowledgments

We thank the chief-scientist, D. Blackman, and the crew from R/V *Melville* (Scripps Institution of Oceanography, UCSD) for providing excellent sampling facilities. We also thank D. Marie for assistance with flow cytometry, and C. de Vargas for inviting us to participate in the cruise. Dr S. Wright graciously provided a new improved version of the Chemtax software (v. 1.95). This work was funded by projects TRANSINDICO (REN2002-10951-E/MAR, MCyT) to R.M. and PicOcean to D.V., and NSF Grant OCE02-21063 to E.G. and M.D. Ohman funded the ship time. F.N. was supported by a doctoral fellowship from the French Research Ministry.

Appendix A. Supplementary materials

Supplementary data associated with this article can be found in the online version at doi:10.1016/j.dsr.2008.06.007.

References

- Adl, S.M., Simpson, A.G.B., Farmer, M.A., Andersen, R.A., Anderson, O.R., Barta, J.R., Bowser, S.S., Brugerolle, G., Fensome, R.A., Fredericq, S., James, L.A., Lodge, J., Lynn, D.H., Mann, D.G., McCourt, R.M., Mendoza, L., Moestrup, O., Mozley-Standridge, S.E., Nerad, T.A., Shearer, C.A., Smirnov, A.V., Spiegel, F.W., Taylor, M.F.J.R., 2005. The new higher level classification of eukaryotes with emphasis on the taxonomy of protists. *Journal of Eukaryotic Microbiology* 52, 399–451.
- Altschul, S.F., Madden, T.L., Schäffer, A.A., Zhang, J., Zhang, Z., Miller, W., Lipman, D.J., 1997. Gapped BLAST and PSI-BLAST: a new generation of protein database search programs. *Nucleic Acids Research* 25, 3389–3402.
- Andersen, R.A., Saunders, G.W., Paskind, M.P., Sexton, J., 1993. Ultrastructure and 18S rRNA gene sequence for *Pelagomonas calceolata* gen. and sp. nov. and the description of a new algal class, the *Pelagophyceae classis* nov. *Journal of Phycology* 29, 701–715.
- Andersen, R.A., Bidigare, R.R., Keller, M.D., Latasa, M., 1996. A comparison of HPLC pigment signatures and electron microscopic observations for oligotrophic waters of the North Atlantic and Pacific Oceans. *Deep Sea Research Part II Topical Studies in Oceanography* 43, 517–537.
- Azam, F., Fenchel, T., Field, J.G., Gray, J.S., Meyer-Reil, L.A., Thingstad, T.F., 1983. The ecological role of water-column microbes in the sea. *Marine Ecology Progress Series* 10, 257–263.
- Bidigare, R., Ondrusek, M.E., 1996. Spatial and temporal variability of phytoplankton pigment distributions in the central equatorial Pacific Ocean. *Deep Sea Research Part II Topical studies in Oceanography* 43, 809–833.
- Biégala, I.C., Not, F., Vaulot, D., Simon, N., 2003. Quantitative assessment of picoeukaryotes in the natural environment using taxon specific oligonucleotide probes in association with TSA-FISH (Tyramide Signal Amplification-Fluorescent *In Situ* Hybridization) and flow cytometry. *Applied and Environmental Microbiology* 69, 5519–5529.
- Brown, S.L., Landry, M.R., Barber, R.T., Campbell, L., Garrison, D.L., Gowing, M.M., 1999. Picophytoplankton dynamics and production in the Arabian Sea during the 1995 southwest monsoon. *Deep Sea Research Part II Topical Studies In Oceanography* 46, 1745–1768.
- Campbell, L., Landry, M.R., Constantinou, J., Nolla, H.A., Brown, S.L., Liu, H., Caron, D.A., 1998. Response of microbial community structure to environmental forcing in the Arabian Sea. *Deep Sea Research Part II Topical Studies in Oceanography* 45, 2301–2325.
- Caron, D.A., 1983. Technique for enumeration of heterotrophic and phototrophic nanoplankton, using epifluorescence microscopy, and comparison with other procedures. *Applied and Environmental Microbiology* 46, 491–498.
- Carreto, J.J., Montoya, N.G., Benavides, H.R., Guerrero, R., Carignan, M.O., 2003. Characterization of spring phytoplankton communities in the rio de la Plata maritime front using pigment signatures and cell microscopy. *Marine Biology* 143, 1013–1027.
- Countway, P.D., Caron, D.A., 2006. Abundance and distribution of *Ostreococcus* sp. in the San Pedro channel, California, as revealed by quantitative PCR. *Applied and Environmental Microbiology* 72, 2496–2506.
- Countway, P.D., Gast, R.J., Dennett, M.R., Savai, P., Rose, J.M., Caron, D.A., 2007. Distinct protistan assemblages characterize the euphotic zone and deep-sea (2500 m) of the western N. Atlantic (Sargasso Sea and Gulf Stream). *Environmental Microbiology* 9, 1219–1232.
- Dandonneau, Y., Montel, Y., Blanchot, J., Giraudeau, J., Neveux, J., 2006. Temporal variability in phytoplankton pigments, picoplankton and coccolithophores along a transect through the North Atlantic and tropical southwestern Pacific. *Deep Sea Research Part II Topical Studies in Oceanography* 53, 689–712.
- Díez, B., Pedros Alió, C., Marsh, T.L., Massana, R., 2001a. Application of denaturing gradient gel electrophoresis (DGGE) to study the diversity of marine picoeukaryotic assemblages and comparison of DGGE with other molecular techniques. *Applied and Environmental Microbiology* 67, 2942–2951.
- Díez, B., Pedros Alió, C., Massana, R., 2001b. Study of genetic diversity of eukaryotic picoplankton in different oceanic regions by small-subunit rRNA gene cloning and sequencing. *Applied and Environmental Microbiology* 67, 2932–2941.
- Díez, B., Massana, R., Estrada, M., Pedros Alió, C., 2004. Distribution of eukaryotic picoplankton assemblages across hydrographic fronts in the Southern Ocean, studied by denaturing gradient gel electrophoresis. *Limnology and Oceanography* 49, 1022–1034.
- DiTullio, G.R., Geesey, M.E., Jones, D.R., Daly, K.L., Campbell, L., Smith, W.O., 2003. Phytoplankton assemblage structure and primary productivity along 170 degrees W in the South Pacific Ocean. *Marine Ecology Progress Series* 255, 55–80.
- Dolven, J.K., Lindqvist, C., Albert, V.A., Bjorklund, K.R., Yuasa, T., Takahashi, O., Mayama, S., 2007. Molecular diversity of alveolates associated with neritic North Atlantic radiolarians. *Protist* 158, 65–76.
- Elwood, H.J., Olsen, G.J., Sogin, M.L., 1985. The small-subunit ribosomal RNA gene sequences from the hypotrichous ciliates *Oxytricha nova* and *Stylonychia pustulata*. *Molecular Biology and Evolution* 2, 399–410.
- Falkowski, P.G., LaRoche, J., 1991. Acclimation to spectral irradiance in algae. *Journal of Phycology* 27, 8–14.
- Fuller, N.J., Campbell, C., Allen, D.J., Pitt, F.D., Zwirgmaier, K., Le Gall, F., Vaulot, D., Scanlan, D.J., 2006a. Analysis of photosynthetic picoeukaryote diversity at open ocean sites in the Arabian Sea using a PCR

- primer biased towards marine algal plastids. *Aquatic Microbial Ecology* 43, 79–93.
- Fuller, N.J., Tarran, G.A., Cummings, D.G., Woodward, M.S., Orcutt, K.M., Yallop, M., Le Gall, F., Scanlan, D.J., 2006b. Molecular analysis of photosynthetic picoeukaryotes community structure along an Arabian Sea transect. *Limnology and Oceanography* 51, 2502–2514.
- Groisillier, A., Massana, R., Valentin, K., Vaulot, D., Guillou, L., 2006. Genetic diversity and habitats of two enigmatic marine alveolate lineages. *Aquatic Microbial Ecology* 42, 277–291.
- Johnson, Z.I., Zinser, E.R., Coe, A., McNulty, N.P., Woodward, E.M.S., Chisholm, S.W., 2006. Niche partitioning among *Prochlorococcus* ecotypes along ocean-scale environmental gradients. *Science* 311, 1737–1740.
- Latasa, M., 2007. Improving estimations of phytoplankton class abundances using Chemtax. *Marine Ecology Progress Series* 329, 13–21.
- Latasa, M., Bidigare, R.R., 1998. A comparison of phytoplankton populations of the Arabian Sea during the Spring Intermonsoon and Southwest Monsoon of 1995 as described by HPLC-analyzed pigments. *Deep Sea Research Part II Topical Studies in Oceanography* 45, 2133–2170.
- Latasa, M., Landry, M.R., Schluter, L., Bidigare, R.R., 1997. Pigment-specific growth and grazing rates of phytoplankton in the central equatorial Pacific. *Limnology and Oceanography* 42, 289–298.
- Latasa, M., Scharek, R., Le Gall, F., Guillou, L., 2004. Pigment suites and taxonomic groups in Prasinophyceae. *Journal of Phycology* 40, 1149–1155.
- Letelier, R.M., Bidigare, R.R., Hebel, D.V., Ondrusek, M.E., Winn, C.D., Karl, D.M., 1993. Temporal variability of phytoplankton community structure based on pigment analyses. *Limnology and Oceanography* 38, 1420–1437.
- Li, W.K.W., 1994. Primary productivity of prochlorophytes, cyanobacteria, and eukaryotic ultraplankton: measurements from flow cytometric sorting. *Limnology and Oceanography* 39, 169–175.
- Longhurst, A., 1998. *Ecological Geography of the Sea*, London.
- López García, P., Rodríguez Valera, F., Pedros Alió, C., Moreira, D., 2001. Unexpected diversity of small eukaryotes in deep-sea Antarctic plankton. *Nature* 409, 603–607.
- Lovejoy, C., Massana, R., Pedros Alió, C., 2006. Diversity and distribution of marine microbial eukaryotes in the Arctic Ocean and adjacent seas. *Applied and Environmental Microbiology* 72, 3236–3244.
- Mackey, M.D., Mackey, D.J., Higgins, H.W., Wright, S.W., 1996. CHEMTAX—a program for estimating class abundances from chemical markers: application to HPLC measurements of phytoplankton. *Marine Ecology Progress Series* 144, 265–283.
- Mackey, D.J., Higgins, H.W., Mackey, M.D., Holdsworth, D., 1998. Algal class abundances in the western equatorial Pacific: estimation from HPLC measurements of chloroplast pigments using CHEMTAX. *Deep Sea Research Part I Oceanographic Research Papers* 45, 1441–1468.
- Marañón, E., Holligan, P.M., Barciela, R., Gonzalez, N., Mourino, B., Pazo, M.J., Varela, M., 2001. Patterns of phytoplankton size structure and productivity in contrasting open-ocean environments. *Marine Ecology Progress Series* 216, 43–56.
- Marie, D., Brussaard, C., Partensky, F., Vaulot, D., 1999. Flow cytometric analysis of phytoplankton, bacteria and viruses. In: Sons, J.W. (Ed.), *Current Protocols in Cytometry*. International Society for Analytical Cytology, pp. 11.11.11–11.11.15.
- Marie, D., Zhu, F., Balague, V., Ras, J., Vaulot, D., 2006. Eukaryotic picoplankton communities of the Mediterranean Sea in summer assessed by molecular approaches (DGGE, TTGE, QPCR). *FEMS Microbial Ecology* 55, 403–415.
- Massana, R., Terrado, R., Forn, I., Lovejoy, C., Pedros-Alió, C., 2006. Distribution and abundance of uncultured heterotrophic flagellates in the world oceans. *Environmental Microbiology* 8, 1515–1522.
- Moon-van der Staay, S.Y., van der Staay, G.W.M., Guillou, L., Vaulot, D., Claustre, H., Medlin, L.K., 2000. Abundance and diversity of Prymnesiophytes in the picoplankton community from the equatorial Pacific Ocean inferred from 18S rDNA sequences. *Limnology and Oceanography* 45, 98–109.
- Moon-van der Staay, S.Y., De Wachter, R., Vaulot, D., 2001. Oceanic 18S rDNA sequences from picoplankton reveal unsuspected eukaryotic diversity. *Nature* 409, 607–610.
- Not, F., Simon, N., Biegala, I.C., Vaulot, D., 2002. Application of fluorescent in situ hybridization coupled with tyramide signal amplification (FISH-TSA) to assess eukaryotic picoplankton composition. *Aquatic Microbial Ecology* 28, 157–166.
- Not, F., Latasa, M., Marie, D., Cariou, T., Vaulot, D., Simon, N., 2004. A single species, *Micromonas pusilla* (Prasinophyceae), dominates the eukaryotic picoplankton in the Western English Channel. *Applied and Environmental Microbiology* 70, 4064–4072.
- Not, F., Massana, R., Latasa, M., Marie, D., Colson, C., Eikrem, W., Pedros Alió, C., Vaulot, D., Simon, N., 2005. Late summer community composition and abundance of photosynthetic picoeukaryotes in Norwegian and Barents Seas. *Limnology and Oceanography* 50, 1677–1686.
- Not, F., Gausling, R., Azam, F., Heidelberg, J.F., Worden, A.Z., 2007. Vertical distribution of picoeukaryotic diversity in the Sargasso Sea. *Environmental Microbiology* 9, 1233–1252.
- Ondrusek, M.E., Bidigare, R.R., Sweet, S.T., Defreitas, D.A., Brooks, J.M., 1991. Distribution of phytoplankton pigments in the North Pacific Ocean in relation to physical and optical variability. *Deep Sea Research Part II Topical Studies in Oceanography* 38, 243–266.
- Raven, J.A., 1998. Small is beautiful: the picophytoplankton. *Functional Ecology* 12, 503–513.
- Reason, C.J.C., Alan, R.J., Lindsay, J.A., 1996. Evidence for the influence of remote forcing on interdecadal variability in the Southern Indian Ocean. *Journal of Geophysical Research* 101, 867–882.
- Rodríguez, F., Derelle, E., Guillou, L., Le Gall, F., Vaulot, D., Moreau, H., 2005. Ecotype diversity in marine picoeukaryote *Ostreococcus* (Chlorophyta, Prasinophyceae). *Environmental Microbiology* 7, 853–859.
- Schlitzer, R., 2007. Ocean Data View, <<http://odv.awi.de>>.
- Sherr, B.F., Sherr, E.B., 2000. Marine microbes: an overview. In: Kirchman, D. (Ed.), *Microbial Ecology of the Oceans*. Wiley-Liss, New York, pp. 13–46.
- Sieburth, J.M., Smetacek, V., Lenz, J., 1978. Pelagic ecosystem structure: heterotrophic compartments of the plankton and their relationship to plankton size fraction. *Limnology and Oceanography* 23, 1256–1263.
- Smith, S.L., Codispoti, L.A., Morrison, J.M., Barber, R.T., 1998. The 1994–1996 Arabian Sea Expedition: an integrated, interdisciplinary investigation of the response of the northwestern Indian Ocean to monsoonal forcing. *Deep Sea Research Part II Topical Studies in Oceanography* 45, 1905–1915.
- Stoeck, T., Zuendorf, A., Breiner, H.-W., Behnke, A., 2007. A molecular approach to identify active microbes in environmental eukaryote clone libraries. *Microbial Ecology* 53, 328–339.
- Stramma, L., Lutjeharms, J.R.E., 1997. The flow field of the subtropical gyre of the South Indian Ocean. *Journal of Geophysical Research* 102, 5513–5530.
- Suzuki, K., Handa, N., Kiyosawa, H., Ishizaka, J., 1997. Temporal and spatial distribution of phytoplankton pigments in the central Pacific Ocean along 175°E during the boreal summers of 1992 and 1993. *Journal of Oceanography* 53, 383–396.
- Suzuki, K., Minami, C., Liu, H., Saino, T., 2002. Temporal and spatial patterns of chemotaxonomic algal pigments in the subarctic Pacific and the Bering Sea during the early summer of 1999. *Deep Sea Research Part II Topical Studies in Oceanography* 49, 5685–5704.
- Thomsen, H.A., Buck, K.R., 1998. Nanoflagellates of the central California waters: taxonomy, biogeography and abundance of primitive, green flagellates (Pedinophyceae, Prasinophyceae). *Deep Sea Research Part II Topical Studies in Oceanography* 45, 1687–1707.
- Thronsen, J., 1976. Occurrence and productivity of small marine flagellates. *Norwegian Journal of Botany* 23, 269–293.
- Utermöhl, H., 1958. Zur Vervollkommnung der quantitativen Phytoplankton-Methodik. *Mitteilungen Internationale Vereinigung für Theoretische und Angewandte Limnologie* 9, 1–38.
- Vaulot, D., Romari, K., Not, F., 2002. Are autotrophs less diverse than heterotrophs in marine picoplankton? *Trends in Microbiology* 10, 266–267.
- Viprey, M., Guillou, L., Ferréol, M., Vaulot, D., 2008. Wide genetic diversity of picoplanktonic green algae (Chloroplastida) uncovered in the Mediterranean Sea by a phylum-specific PCR approach. *Environmental Microbiology* 10, 1804–1822.
- Worden, A.Z., Not, F., 2008. Ecology and diversity of picoeukaryotes. In: Kirchman, D.L. (Ed.), *Microbial Ecology of the Ocean*. Wiley, pp. 159–205.
- Worden, A.Z., Nolan, J.K., Palenik, B., 2004. Assessing the dynamics and ecology of marine picophytoplankton: the importance of the eukaryotic component. *Limnology and Oceanography* 49, 168–179.
- Wright, S.W., Jeffrey, S.W., 2006. Pigment markers for phytoplankton production. In: Volkman, J.K. (Ed.), *Handbook Environmental Chemistry*, vol. 2. Springer, Berlin, Heidelberg, pp. 71–104.
- Yuan, J., Chen, M.-Y., Shao, P., Zhou, H., Chen, Y.-Q., Qu, L.-H., 2004. Genetic diversity of small eukaryotes from the coastal waters of Nansha Islands in China. *FEMS Microbiology Letters* 240, 163–170.
- Zhu, F., Massana, R., Not, F., Marie, D., Vaulot, D., 2005. Mapping of picoeukaryotes in marine ecosystems with quantitative PCR of the 18S rRNA gene. *FEMS Microbial Ecology* 52, 79–92.
- Zubkov, M.V., Sleigh, M.A., Tarran, G.A., Burkill, P.H., Leakey, R.J.G., 1998. Picoplanktonic community structure on an Atlantic transect from 50°N to 50°S. *Deep Sea Research Part I Oceanographic Research Papers* 45, 1339–1355.